Potential of low molecular weight gelling agent *N*-palmitoyl-glycyl-histidine (Pal-GH) as a new component of topically applied gel formulation

2019

Sabrina

Josai University
Graduate School of Pharmaceutical Sciences
Laboratory of Pharmaceutics and Cosmeceutics

TABLE OF CONTENTS

ABBREVIATIONS

Pal-GH	*N*-palmitoyl-glycyl-histidine
IVM	ivermectin
MTZ	metronidazole
PBS	phosphate buffered saline
m.w.	molecular weight
PG	propylene glycol
DMSO	dimethyl sulphoxide
IPM	isopropyl myristate
GS	gel spray
CPE	chemical penetration enhancer
ETOH	ethanol
F2.5	Pal-GH 2.5%
$F2.5_{2.5GL}$	Pal-GH 2.5%, glycerin 2.5%
$F2.5_{10GL}$	Pal-GH 2.5%, glycerin 10%
$F2.5_{4PG}$	Pal-GH 2.5%, propylene glycol 4%
$F2.5_{IVM}$	Pal-GH 2.5%, ivermectin 0.1%
$F2.5_{2.5GL-IVM}$	Pal-GH 2.5%, glycerin 2.5%, ivermectin 0.1%
$F2.5_{10GL-IVM}$	Pal-GH 2.5%, glycerin 10%, ivermectin 0.1%
$F2.5_{4PG-IVM}$	Pal-GH 2.5%, propylene glycol 4%, ivermectin 0.1%
F5	Pal-GH 5%
$F5_{2.5GL}$	Pal-GH 5%, glycerin 2.5%
$F5_{10GL}$	Pal-GH 5%, glycerin 10%
$F5_{4PG}$	Pal-GH 5%, propylene glycol 4%
$F5_{IVM}$	Pal-GH 5%, ivermectin 0.1%
$F5_{2.5GL-IVM}$	Pal-GH 5%, glycerin 2.5%, ivermectin 0.1%
$F5_{10GL-IVM}$	Pal-GH 5%, glycerin 10%, ivermectin 0.1%
$F5_{4PG-IVM}$	Pal-GH 5%, propylene glycol 4%, ivermectin 0.1%
$F2.5_{MTZ}$	Pal-GH 2.5%, metronidazole 1%
$F5_{MTZ}$	Pal-GH 5%, metronidazole 1%
$F5_{IPM-MTZ}$	Pal-GH 5%, isopropyl myristate 10%, metronidazole 1%

$F5_{PG\text{-}MTZ}$	Pal-GH 5%, propylene glycol 4%, metronidazole 1%
$F5_{DMSO\text{-}MTZ}$	Pal-GH 5%, dimethyl sulphoxide 5%, metronidazole 1%
$F5_{EtOH\text{-}MTZ}$	Pal-GH 5%, ethanol 20%, metronidazole 1%
$F5_{TRANS\text{-}MTZ}$	Pal-GH 5%, diethylene glycol monoethyl ether 10%, metronidazole 1%
$F10_{MTZ}$	Pal-GH 10%, metronidazole 1%
IPM_{MTZ}	isopropyl myristate 10%, metronidazole 1% (in aqueous solution)
PG_{MTZ}	propylene glycol 4%, metronidazole 1% (in aqueous solution)
$DMSO_{MTZ}$	dimethyl sulphoxide 5%, metronidazole 1% (in aqueous solution)
$EtOH_{MTZ}$	ethanol 20%, metronidazole 1% (in aqueous solution)
$TRANS_{MTZ}$	transcutol 10%, metronidazole 1% (in aqueous solution)

Abstract

Development of new pharmaceutical additives is very important to widen and increase good pharmaceutical products. *N*-palmitoyl-glycyl-histidine (Pal-GH) can be a new low molecular weight gelling agent. Only a few low molecular gelling agents were reported, although many natural and synthetic high molecular gelling agents have already been in the market. Pal-GH exhibited thixotropic behavior, low viscosity, and high dissolving properties for a wide range of hydrophilic to lipophilic drugs similar to those in high molecular gelling agents. Ivermectin (IVM) and metronidazole (MTZ) were selected as hydrophilic and lipophilic model drugs in this study.

Orally administered IVM has been used to treat the scabies. However, this treatment is associated with well-known side effects, thus this study is anticipated to search for alternative routes of administration. Although a topical formulation of IVM could be a candidate, it requires whole body application except the head and face for several hours on a daily basis. Thixotropic is an essential property for applying, spreading, and expanding the material while retaining its appearance and form. It is an important consideration in preparing a gel spray formulation. Then, the author prepared Pal-GH gel spray formulations from its aqueous solution by a heating and cooling method in order to be supplied to the scabies treatment in the first part of the present study.

Rheological behavior and physical appearance (spraying, spreading ability, volume of spraying, and homogeneity) of the prepared formulations were evaluated. Pal-GH gel with propylene glycol (PG) demonstrated impressive rheological properties (typical thixotropic behavior) with high hysteresis area and high spreading ability among all the tested Pal-GH gels. The obtained IVM concentration in skin after topical application of 0.1% IVM in Pal-GH formulation onto the hairless rat skin was extremely higher than the reported therapeutic concentration obtained from oral administration in humans. These results suggested that topical application of IVM using a Pal-GH gel spray formulation could be an alternative to the conventional oral forms for the scabies treatment.

The author tried to increase the skin permeation of metronidazole (MTZ), a hydrophilic drug unlike a typical lipophilic compound, IVM, after the topical application of Pal-GH gel, since the skin permeation rate of water-soluble drugs is low in general in the second part of this study. A combined effect of chemical penetration-enhancers (CPEs), such as isopropyl myristate (IPM), PG, ethanol (EtOH), diethylene glycol monoethyl ether (transcutol®, TRANS), and dimethyl sulfoxide (DMSO), was evaluated on the skin permeation of MTZ. Three-dimensional network structure of Pal-GH gel and its combination with several CPEs was also evaluated, to find out a relation between the rheological properties and skin penetration-enhancing effects. As results, 5% Pal-GH gel containing 1% MTZ ($F5_{MTZ}$) exhibited a 2.7-fold higher MTZ permeation through excised hairless rat skin than its solution. Furthermore, Pal-

GH 5% with PG 4% ($F5_{PG\text{-}MTZ}$) and Pal-GH 5% with IPM 10% ($F5_{IPM\text{-}MTZ}$) further increased the skin permeation of MTZ when compared to $F5_{MTZ}$. Interestingly, $F5_{PG\text{-}MTZ}$ markedly increased the skin penetration of MTZ, although no enhancement effect was observed by MTZ PG solution (PG_{MTZ}). Thus, Pal-GH formulations containing PG or IPM enhanced the skin permeation of MTZ, suggesting usefulness of Pal-GH gel to improve the skin permeation of hydrophilic drugs.

The microstructure of the Pal-GH formulations were observed by light microscopy and TEM. $F5_{PG\text{-}MTZ}$, Pal-GH 5% with DMSO 5% ($F5_{DMSO\text{-}MTZ}$) and Pal-GH 5% with EtOH 20% ($F5_{EtOH\text{-}MTZ}$) showed a highly dense and thick fibrous structure compared with those in $F5_{MTZ}$ and $F5_{MTZ}$ containing the other CPEs. $F5_{MTZ}$, $F5_{EtOH\text{-}MTZ}$ and $F5_{TRANS\text{-}MTZ}$ showed homogeneous and straight fibrous structures. Fragmented fibrous structures were also observed in $F5_{EtOH\text{-}MTZ}$ and $F5_{TRANS\text{-}MTZ}$. On the other hand, $F5_{IPM\text{-}MTZ}$, $F5_{PG\text{-}MTZ}$ and $F5_{DMSO\text{-}MTZ}$ showed straight, but twisted fibrous structures. These results suggest that structural differences such as higher amount of fibers and disconnected fibers may be related to the skin penetration enhancement effect of the entrapped drug in the Pal-GH gel formulation. Thus, highly dense and twisted fibrous structures were correlated with thixotropic behavior of Pal-GH gel formulations.

General Introduction

Gel spray (GS) formulation is a semi-solid formulation containing a gelling agent with thixotropic behavior and can be sprayed with a mechanical pump. It has many advantages compared to conventional topical preparation, such as an approach for application to large skin areas with a single spray application without further contact with the applied formulation. Compared to inconveniences of a bath formulation, GS still has many merits. It has long duration of exposure to the skin and uses smaller amount of drug, hence cost effective. Gelling agent having thixotropic behavior is an important consideration in preparing a gel spray formulation. It exhibits an isothermal system in which apparent viscosity decreases under shear stress, followed by a gradual recovery when the stress is removed. It is an essential property in applying, spreading, and expanding the material while retaining its appearance and form. Thixotropic gels can also be applied on a wider range of skin for a long period.

Gelators are materials that are capable of turning a liquid solvent into a "solid-like" substances by entrapping and immobilizing the solvent molecules at macroscopic level, and they are used to obtain gels via the process of gelation. Based on their source, gels can be classified into natural gels and artificial (synthetic) gels. Based on constitution, artificial gels can be further classified into macromolecular (polymeric) gels (this is major) and low molecular gels (this is minor). Finally, based on the interaction within the 3D network,

macromolecular gels can be subdivided into chemically cross-linked gels and physically crosslinked gels, whereas the low molecular gels are normally physically cross-linked. Gels formed by chemical cross-linking (strong covalent bond) cannot be re-dissolved and are not thermo-reversible, whereas gels formed by physical interaction (weak non covalent interactions) can be re-dissolved and are thermo-reversible.

N-palmitoyl-glycyl-histidine (Pal-GH) is a novel low molecular weight gelling agent. Therefore, it can be redissolved and thermoreversible. It has valuable properties like thixotropic behavior, lower viscosity and high dissolving properties for a wide range of hydrophilic to lipophilic drugs. Pal-GH cannot only be used as a base for GS formulation due to its thixotropic properties, but also expected as a good enhancer [1, 2]. Since the percutaneous absorption rates of water-soluble drugs are generally low, an enhancing system is needed when using the skin as an administration site for the drugs.

Skin is utilized as an application site for many topical and transdermal drug delivery systems. The stratum corneum (SC), barrier property layer, poses a formidable challenge to formulators of transdermal drug delivery system which need the modification for enhancing the skin permeation of poorly penetrating drugs like water soluble drug [3, 4]. In order to overcome the high barrier function in the stratum corneum in delivering these drugs, several chemical enhancers had already evaluated to promote their skin permeation. The contribution of Pal-GH on the skin permeation of metronidazole (MTZ), and synergistic effect of its

combination with some enhancers like propylene glycol (PG), ethanol (EtOH), isopropyl myristate (IPM), diethylene glycol monoethyl ether (Transcutol®) and dimethyl sulfoxide (DMSO) has not been studied.

General concepts of this research are to design a GS formulation showing thixotropic properties, and to observe the effects of Pal-GH gel formulation and its combination with several CPEs on the skin permeation and skin concentration of topically applied hydrophilic and lipophilic model drugs. Thus, the design to use Pal-GH as a gelling agent for topically applied GS formulation containing ivermectin (IVM) as a lipophilic model drug to treat scabies and also as enhancer for MTZ (hydrophilic model drug) for scabies and rosacea/acne treatment, respectively. Then, the understanding of the microstructures of Pal-GH in influencing thixotropic properties, enhancing skin permeation and skin concentration of the model drugs will be essential in developing superior topical formulations.

This study is divided in two chapters as follows: In chapter 1, designing of a topically applied GS formulation with IVM using Pal-GH was determined. GS formulation containing IVM was an ideal formulation to treat scabies, since it has fewer side effects compared to oral IVM and easier for whole body application. Hence, several physical and rheological properties, release, skin permeation and skin concentration of IVM have been studied to produce an impressive topical GS formulation.

In chapter 2, Pal-GH and its combination with several enhancers was investigated for its ability to enhance skin permeation and concentration of MTZ. MTZ is one of a nitro imidazole derivative and was expected to skin enrichment for therapeutics of the acne and rosacea. Studies of topical administration of MTZ were promising, since only a minimal amount of the active agent reached the skin. Also, considerable side effects were observed following oral administration. For topical drugs, the emphasis on its skin concentration is greater compared to its skin permeation since it has a direct correlation on its efficacy and safety of active compound. Therefore, skin permeation and skin concentration of MTZ from Pal-GH gel formulation and its combination with several enhancers were evaluated. In addition, microstructural observation of Pal-GH gel formulation showing thixotropic properties, and enhanced skin permeation and concentration of drugs were also evaluated. The microstructural properties of the supramolecular gel affects to its rheological properties, skin permeation and concentration enhancement of lipophilic and hydrophilic drugs. Fibrous structures were evaluated for Pal-GH and its combination with several enhancers. Microscopic, and TEM observation were conducted to explain this microstructural changes in the GS formation.

Chapter 1

Design of topically applied gel-spray formulation of ivermectin using a novel low molecular gelling agent, *N*-palmitoyl-glycyl-histidine (Pal-GH) to treat Scabies

1.1. Introduction

Gelling agents are capable of turning liquids into "solid-like" substances by entrapping and immobilizing solvent molecules at a macroscopic level [5]. They can be classified into polymeric macromolecular (>10 kDa) or low molecular weight (<10 kDa) gelling agents. Several kinds of low molecular weight building blocks can self-assemble to form one-dimensional nanofibers, and then three-dimensional entanglement of the nanofibers causes gelation of the solvents. Such hydrophilic supramolecular gelling agents can be designed at the molecular level depending on their proposed use, because of their relatively simple molecular structure [6,7]. The biocompatibility and biodegradability of these gels make them ideal for drug delivery systems [8]. In contrast to conventional polymeric gels, such supramolecular gels are characterized by the reversible transition between sol and gel states.

N-palmitoyl-glycyl-histidine (Pal-GH) is a unique molecule with hydrophilic and hydrophobic moieties consisting of glycine and histidine, and palmitic acid, respectively (Fig. 1) [2]. In spite of its weak strength compared with conventional and marketed polymer gels,

the high controllability of the molecular structure and function has led to a new gel substrate. Pal-GH can be gelled at a broad range of concentrations and even at a low level. Pal-GH has valuable properties such as thixotropic behavior, lower viscosity, and high dissolving properties for a wide range of hydrophilic to lipophilic drugs. Thixotropic behavior is an important consideration in preparing a gel spray formulation.

Oral administration of ivermectin (22,23-dihydroavermectin B1a; IVM) is presently used world-widely in scabies therapy. Scabies (a parasitic roundworm infection) is a major worldwide public health problem in many developing countries [9], and it has become a major problem even in Japan and other developed countries due to highly aged societies. Curing the parasitic infection helps to improve quality of life (QOL) for patients. In people with weakened immune systems, curing the roundworm infection can reduce the risk of developing a severe or life-threatening infection. IVM belongs to a class of drugs known as anthelmintics, and it works by its paralyzing and killing the parasites. IVM is considered to be absorbed into the systemic circulation and distributed to the skin tissues through sebaceous glands after oral administration. Hass *et al.* (2002) reported that IVM concentration in the stratum corneum ranged from 40 to 80 ng/g in scabies patients who took 12 mg oral IVM, which is regarded as an effective dose [10]. However, this treatment for scabies is potentially hazardous and associated with moderate to severe side effects for caregivers as well as patients [11, 12].

Furthermore, the safety and efficacy of oral IVM have not been well-established, especially in older patients with impaired liver function, in children, and in pregnant women [12, 13].

Such side effects related to oral IVM prompted medical and pharmaceutical researchers to investigate alternative routes of administration and novel formulations, such topically applied cream, gel, or foam for whole body bathing as a safe and simplified therapy [14]. These topical preparations probably function through IVM absorption through the skin barrier to the diseased sites with fewer systemic adverse effects than oral formulations. Thus, such topical formulations of IVM are candidate treatments. However, they still require whole-body application for several hours on a daily basis to maintain effective IVM concentrations in the skin of scabies patients.

The author was surprised to observe in preliminary experiment that topical skin application of 0.1% IVM solution provided much higher concentrations in the stratum corneum at the application site compared with the effective concentration reported by Hass *et al.* (2002). However, scabies spreads easily by infestation both by direct skin-to-skin contact and by contamination through clothing, bedding, and furniture [15-17]. Therefore, I decided to study gel spray (GS) formulations that could cover a large skin area in a single application without further contact with the applied formulation. Pal-GH and IVM were selected as a gelling agent for a GS formulation and lipophilic model drug respectively, to be available for scabies treatment.

Compound	Chemical structure	*M.W.*
N-palmitoyl-glycyl-histidine (Pal-GH)	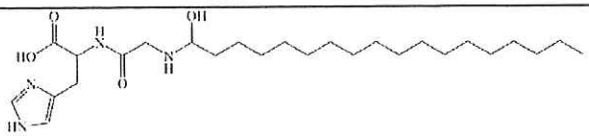	564.0
Propylene glycol alginate (PGA)	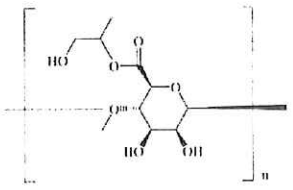	—
Ivermectin (IVM)	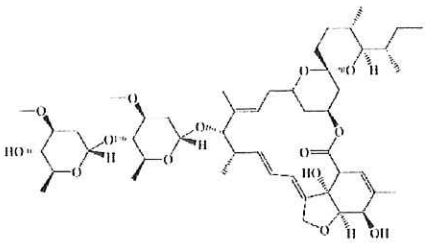	875.1
Propylene glycol (PG)		76.1

Fig. 1. Chemical structures of Pal-GH, PGA, IVM and PG, respectively. clog *P* value of ivermectin is 5.83.

Thixotropic behavior is necessary to prepare a GS formulation, because it exhibits an isothermal system, in which apparent viscosity decreases under shear stress, followed by a gradual recovery when the stress is removed [18]. Thus, the main objective of this work was to design a topically applied Pal-GH formulation containing IVM. The formulation was prepared by a heating-and-cooling method. The rheological properties and physicochemical evaluation of the prepared Pal-GH GS formulations were determined. The skin concentration and IVM-release properties were also determined.

Hairless rat skin has been used as a good alternative membrane for human skin to evaluate skin permeation profiles and the permeability coefficients of drugs [19–22]. Moreover, as the availability of sufficient human skin for skin permeation studies is usually unavailable due to ethical issues, hairless rat skin was used in the present study

1.2. **Materials and methods**

1.2.1. Materials

Pal-GH premix (composed of 6% Pal-GH, 30% 1,2-octanediol, 20% 1,3-butanediol, 2% polyoxyethylene lauryl ether, 1% stearic acid, and 41% purified water) and propylene glycol alginate (PGA) were obtained from Nissan Chemical Industries, Ltd. (Tokyo, Japan). IVM was purchased from Tocris Bioscience (Bristol, U.K.), and glycerin (GL) and propylene glycol (PG) were from Kanto Chemical Co., Inc. (Tokyo, Japan). Sucrose was purchased from Wako Pure Chemical Industries, Ltd. (Osaka, Japan). Other chemicals and reagents were of special grade or HPLC grade (purchased from Wako Pure Chemical Industries, Ltd.) and used without further purification.

1.2.2. Animal

Male hairless rats (200–250 g) were purchased either from Life Science Research Center, Josai University (Sakado, Saitama, Japan) or Ishikawa Experiment Animal

Laboratories (Fukaya, Saitama, Japan). The animals were housed in temperature-controlled rooms (25 ± 2°C) with a 12 h light-dark cycle (7:00–19:00 h), and were allowed free access to food (Oriental Yeast Co., Tokyo, Japan) and tap water. All breeding procedures and the experiments on animals were performed in accordance with the guidelines of the Animal Experiment Committee of Josai University.

1.2.3. Preparation of Pal-GH formulations

The Pal-GH formulations were prepared by a heating-and-cooling method as follows (Fig. 2): Pal-GH premix was dissolved in purified water at 85°C. Then, 0.1% IVM was completely dissolved into the Pal-GH solution at 75°C, followed by adding PG or GL at different concentrations.

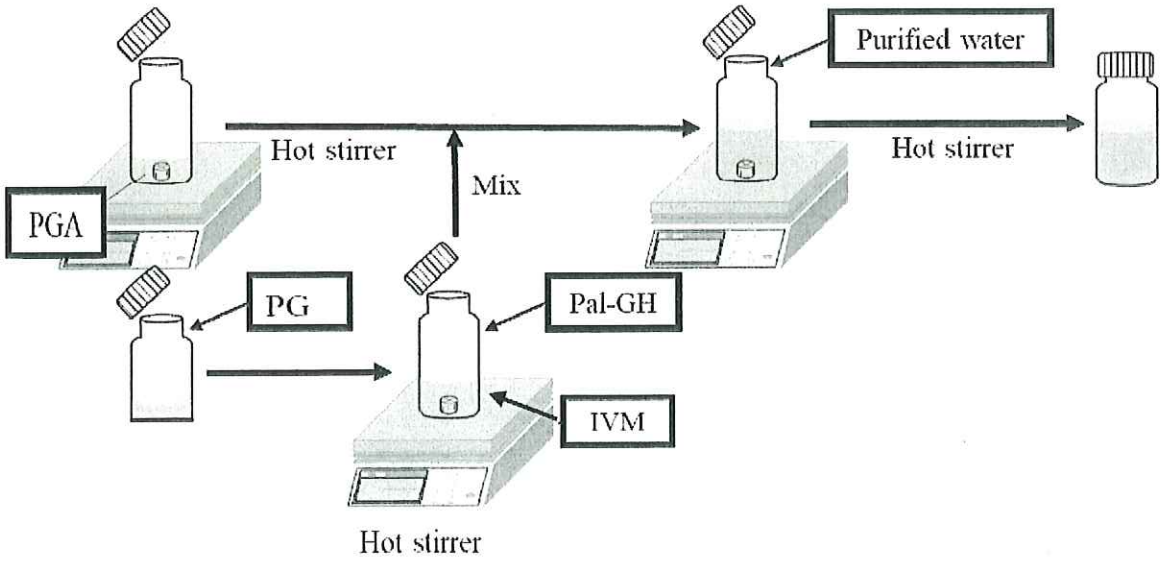

Fig. 2. Scheme of Pal-GH gel preparation

Furthermore, PGA aqueous solution was obtained by stirring in purified water at 85°C for 1 h as stabilizer and thickener. The obtained PGA solution was mixed with the Pal-GH solution containing IVM at 1,000 rpm at 75°C for 1 h (until homogeny). After mixing, the formulation was kept at room temperature before use. Pal-GH gel formulations without IVM were also prepared by mixing the Pal-GH solution containing GL or PG and the PGA solution at 1,000 rpm at 75–85°C for 1 h. Fig. 2 and Table 1 shows the scheme Pal-GH gel preparation and the compositions of the Pal-GH formulations.

Table 1. Composition and codes of the prepared Pal-GH gel formulations

Pal-GH conc. (premix)	Additives	Formulation code without IVM	Formulation code containing 0.1% IVM
2.5%	No additive (base)	F2.5	$F2.5_{IVM}$
	Glycerin 2.5%	$F2.5_{2.5GL}$	$F2.5_{2.5GL\text{-}IVM}$
	Glycerin 10%	$F2.5_{10GL}$	$F2.5_{10GL\text{-}IVM}$
	Propylene glycol 4.0%	$F2.5_{4PG}$	$F2.5_{4PG\text{-}IVM}$
5.0%	No additive (base)	F5	$F5_{IVM}$
	Glycerin 2.5%	$F5_{2.5GL}$	$F5_{2.5GL\text{-}IVM}$
	Glycerin 10%	$F5_{10GL}$	$F5_{10GL\text{-}IVM}$
	Propylene glycol 4.0%	$F5_{4PG}$	$F5_{4PG\text{-}IVM}$

1.2.4. Physical characterization of Pal-GH formulations

Physical characterization of the Pal-GH formulations was performed, including solid-like behavior, spraying ability, spread area, weight, and homogeneity of a single spray application. The solid-like behavior of these formulations before and after shaking was evaluated visually. Spraying ability of Pal-GH formulation was evaluated using a general

spraying nebulizer (Toki Mini Spray PET vol. 20 mL, 0.35 mm i.d. nozzle, Sansho, Tokyo, Japan), and the sprayed area on a glass plate from a vertical distance of 15 cm from the nozzle to the plate was measured using imaging software (cellSens, Olympus Corp., Tokyo, Japan) and using a stereoscopic microscope (SZ61, Olympus Corp.). The weight of a single application of each sprayed formulation was measured by weighing the sample on the glass plate. Aggregation of the sprayed formulations after drying was observed to evaluate homogeneity. Moreover, a flow-ability test was conducted by spraying each Pal-GH formulation from a distance of 15 cm from the nozzle to a vertical glass plate (Fig. 3). Movement of the sprayed formulation was observed using the naked eye for 1minute.

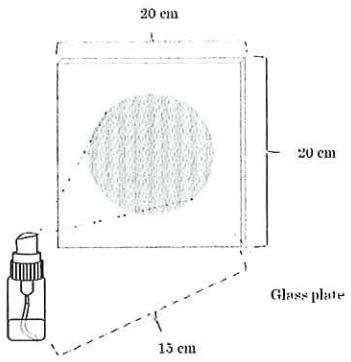

Fig. 3. Evaluation of spraying area of prepared formulations.

1.2.5. Evaluation of the rheological properties of Pal-GH formulations

The rheological properties (thixotropic properties and viscosity) of Pal-GH formulations were evaluated using a rotational viscometer (Toki Sangyo Co., Ltd., Tokyo,

Japan). The measurement conditions were as follows (Table 2): the temperature was maintained at 25°C and 32°C, corn rotor was 3° × R14, sample volume was 0.4 mL, rotation speed was increased from 0 to 100 rpm over 20 min (1200 s) and decreased from 100 to 0 rpm over the same period (Fig. 4), and a flow analysis method was used. The viscosities of the Pal-GH gel formulations and sucrose solutions were evaluated. Moreover, the shear thinning of Pal-GH gel bases was evaluated by measuring their viscosity at different shear rates (0–200 s^{-1}). Hysteresis area was calculated by using VA 2000 software (Toki Sangyo Co., Ltd).

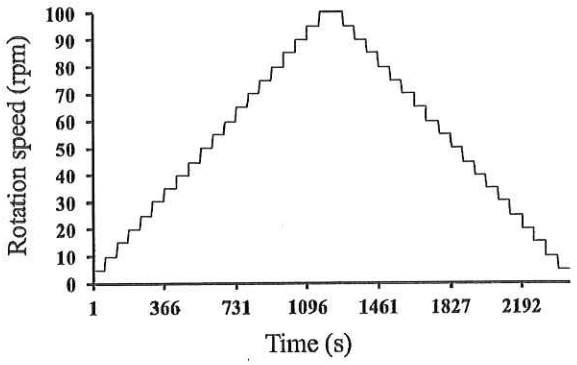

Fig. 4. Program step of rotating viscometer.

Table 2. Rotating viscometer condition.

Apparatus	Viscometer RE-215H
Temperature	25°C
Corn rotor	3° × R14
Sample volume	0.4 mL
Measurement mode	Program step
Analysis method	Flow analysis

1.2.6. FTIR measurement of Pal-GH formulation

FT-IR spectra were measured for selected Pal-GH formulations. Samples were analyzed to confirm the interaction between IVM and Pal-GH. All spectra were recorded by FT-IR with single-reflection ATR using a diamond prism (IRT Tracer-100, Shimadzu Corporation, Kyoto, Japan) in the range of 400–4,000 cm^{-1} with 4 cm^{-1} steps and 40 scans.

1.2.7. IVM release from Pal-GH formulations

IVM release from the formulations was evaluated for selected Pal-GH formulations. This experiment was performed using a side-by-side diffusion cell (effective diffusion area: 0.95 cm^2) with a sheet of dialysis membrane (molecular weight cut-off; 2,000–14,000 Da) (Sanko Junyaku Co., Tokyo, Japan) over 24 h. The sample (0.30 g) was spread evenly in a glass cell compartment with a 0.3 mL volume and set on the membrane, and the receptor compartment was filled with 3.0 mL of soybean oil because of the high lipophilicity of IVM. The receptor cell was agitated using a magnetic stirrer throughout the experiment. The temperature in the receiver compartment was kept at 32°C using a thermostatic water bath circulating through the double glass walls of the diffusion cell. Aliquots (0.50 mL) were withdrawn from the receptor compartment at predetermined times, and the same volume of fresh medium was replaced to maintain the receiver volume. The extraction ratio of IVM from soybean oil was obtained to calculate its exact concentration.

1.2.8. Skin permeation and concentration of ivermectin

Full thickness hairless rat skin was excised from the abdomen under anesthesia by *i.p.* injection of the three types of anesthesia (medetomidine, 0.375 mg/kg; butorphanol, 2.5 mg/kg; and midazolam, 2 mg/kg). Excess fat was trimmed off, and the excised skin was set in a Franz diffusion cell (effective diffusion area: 1.77 cm^2) with the epidermis side facing the donor compartment. Phosphate buffered saline (PBS), pH 7.4, was added to the receiver compartments. The experiments using the skin were conducted after hydration with PBS for 60 min. The Pal-GH formulation containing 0.1% IVM (1.0 mL) was loaded into the donor compartment (epidermal side). The receiver solution was agitated using a stirrer bar and a magnetic stirrer throughout the experiments. The diffusion cells were kept at 32°C with a water jacket connected to a water bath. In addition, at the end of the experiment (24 h) the amount of IVM that permeated through the skin was also determined, an aliquot (0.50 mL) was withdrawn from the receiver chamber. Then, the applied formulation was gently removed using a cotton swab and the skin sample was washed 20 times with 1.0 mL PBS. The permeation area of the skin was then cut into small pieces after gentle removal of excess water on the skin using Kimwipes® paper.

IVM concentrations in full-thickness skin and viable epidermis and dermis (VED) were determined, and the amount of IVM in the stratum corneum was calculated by subtraction of

its amount in the VED from that in full-thickness skin. Then, the IVM concentration in the stratum corneum was estimated under the assumption that the density of the stratum corneum would be 1.2 g/cm^3 [23]. The IVM concentration in VED was obtained by 20 repetitions of stripping of the stratum corneum layers from the full-thickness skin using adhesive tape (Cellotape®, Nichiban, Tokyo, Japan) just after finishing the washing process.

1.2.9. Determination of IVM

IVM concentration in soybean oil: methanol (200 μL) was added to each soybean oil solution (200 μL), and the obtained mixture was vortexed for 10 min and centrifuged twice for 5 min to obtain the supernatant. The supernatant (100 μL) was used for high-performance liquid chromatography (HPLC) assays.

Skin concentration: the obtained skin piece (0.05 g) was minced using scissors and homogenized (4°C, 5 min) with 0.45 mL of methanol for 2.5 min using a homogenizer (Polytron PT-MR 3000; Kinematica Inc., Littau, Switzerland). Methanol (0.5 mL) was added and homogenized again for 2.5 min, then agitated for 15 min. After centrifugation (5,000 rpm, 4°C, 5 min), the supernatant (100 μL) was mixed with the same volume of methanol then agitated and centrifuged again using the same conditions. The obtained supernatant (100 μL) was injected into the HPLC system, and the measurement was obtained using the same conditions as described below.

The HPLC system (Shimadzu Corporation) consisted of a system controller (CBM-20A), pump (LC-20AD), auto-sampler (SIL-20AC), column oven (CTO-20A), UV detector (SPD-M20A), and analysis software (LC Solution). The column was an Inertsil® ODS-3 (5 μm, 4.6 × 250 mm) (Nihon Waters K.K.; Tokyo, Japan), which was maintained at 40°C. The mobile phase was acetonitrile : methanol : water = 6 : 3 : 1 (0–12 min). The flow rate was adjusted to 1.0 mL/min. IVM was detected at 245 nm.

1.2.10. Statistical analysis

Statistical analysis for the amount of skin concentration of IVM and *in vitro* release of IVM were performed using Student's *t*-test, and *P* value less than 0.05 were considered to be significant.

1.3. Results

1.3.1. Physical properties of Pal-GH gel formulation.

Fig. 5 shows photographs of the Pal-GH gel formulation before (Fig. 5a) and after (Fig. 5b) shaking the bottles to evaluate the ability to form a tight gel. Only the results of $F2.5_{4PG\text{-}IVM}$ are displayed as examples.

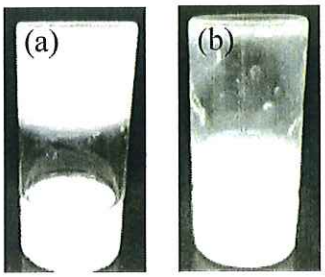

Fig. 5. Photographs of solid-like behavior of Pal-GH gel formulation before (a) and after shaking (b). The Pal-GH gel shows a tight gel (solid like) before shaking, and then a sol just after shaking

Table 3 summarizes the results of the physical characterizations (gel-forming property after shaking, spraying ability, sprayed area, weight of sprayed formulation, and homogeneity) of 18 Pal-GH formulations with 2.5% and 5% Pal-GH premix in different additives and with and without IVM. When spraying these formulations, almost the same weight (0.15–0.22 g) could be sprayed using a general spraying nebulizer (Toki Mini Spray PET, details in the experimental section) independent of the formulations. Most of the formulations showed a sol-gel transition behavior before and after shaking (see Fig. 5). In addition, the sprayed areas were dependent on the formulation, although all formulations could be sprayed using the nebulizer. Larger sprayed areas were observed in most F5 formulations, except for F5 and $F5_{IVM}$. On the other hand, the sprayed areas obtained from the F2.5 formulations were smaller than those obtained from the F5 formulations. Furthermore, the homogeneity of the sprayed formulations was also evaluated. All formulations showed good homogeneity, and almost the same weight

of formulation was sprayed from the nebulizer. No aggregation spots were observed in the sprayed area after drying (data not shown).

Table 3. Physical properties of Pal-GH gel formulations

Sample code	Gel form after shaking	Spraying ability	Sprayed area (cm^2)	Weight of sprayed formulation (g) (n=3)	Homogeneity
F2.5	o	o	50.5	0.150 ± 0.02	o
$F2.5_{2.5GL}$	o	o	153.86	0.186 ± 0.01	o
$F2.5_{10GL}$	o	o	176.625	0.190 ± 0.017	o
$F2.5_{4PG}$	o	o	113.04	0.190 ± 0.01	o
$F2.5_{IVM}$	o	o	38.46	0.215 ± 0.05	o
$F2.5_{2.5GL\text{-}IVM}$	o	o	54.4	0.193 ± 0.006	o
$F2.5_{10GL\text{-}IVM}$	o	o	63.58	0.197 ± 0.006	o
$F2.5_{4PG\text{-}IVM}$	o	o	91.2	0.190 ± 0.005	o
F5	o	o	38.46	0.156 ± 0.01	o
$F5_{2.5GL}$	o	o	145.19	0.186 ± 0.01	o
$F5_{10GL}$	o	o	171.9	0.180 ± 0.02	o
$F5_{4PG}$	o	o	132.6	0.187 ± 0.02	o
$F5_{IVM}$	o	o	38.46	0.190 ± 0.037	o
$F5_{2.5GL\text{-}IVM}$	o	o	132.6	0.186 ± 0.02	o
$F5_{10GL\text{-}IVM}$	o	o	153.86	0.186 ± 0.015	o
$F5_{4PG\text{-}IVM}$	o	o	132.6	0.170 ± 0.05	o

Symbols; ○: confirmed gel forming, spraying ability, or homogeneity. ×: not confirmed
The sprayed area on a glass plate was measured using imaging software after spraying at a vertical distance of 15 cm from the plate. Weight of sprayed formulation was measured to evaluate the amount of one spray.

Moreover, suitable viscosity for easy of spraying and flow-ability of the sprayed formulation on skin were determined qualitatively using different concentrations of sucrose, to facilitate the determination of viscosity, because sucrose solutions show a typical Newtonian flow. Table 4 summarizes the spraying ability, spread-ability, and flow-ability of the Pal-GH formulations on skin as a function of viscosity. As a result, viscosity ranging between 51 and 250 mPa·s was considered to be suitable for topical application using spray formulations. In addition, the highest viscosity that was easily sprayed using a general spraying nebulizer was

determined to be 250 mPa·s, and the lowest viscosity in which the vehicle maintained the sprayed area on the skin was 51 mPa·s.

Table 4. Evaluation of spraying ability, spread-ability, and flow-ability measured by sucrose solutions

Viscosity range (mPa·s)	Spraying ability	Spread-ability	Flow-ability on skin
1–10	Spraying possible	>400 cm^2	Spread over the sprayed area by flowing down of the formulation
11–50	Spraying possible	100–400 cm^2	Flowing down of the formulation
51–250	Spraying possible	<100 cm^2	Maintained across the sprayed area over the time
251–400	Leakage only	No spread-ability	Maintained across the sprayed area over the time
>400	Impossible to spray	No spread-ability	Maintained across the sprayed area over the time

All observations were done using sucrose viscous solutions

1.3.2. Thixotropic properties and viscosity of Pal-GH gel formulations

The thixotropic properties of the Pal-GH gel formulations were further investigated. Fig. 6 shows rheograms of several Pal-GH gel formulations at Pal-GH concentrations of 2.5% (Fig. 6a) and 5% (Fig. 6b). Closed and open symbols indicate increasing shear rate and decreasing shear rate, respectively. Thixotropic behavior was clearly observed in all formulations containing IVM (Fig. 6). The hysteresis area of these F2.5 and F5 changed with the Pal-GH premix concentration as well as with the addition of IVM and PG or GL to the formulation. Among the formulations, higher hysteresis areas were observed in $F2.5_{4PG\text{-}IVM}$ and $F5_{4PG\text{-}IVM}$, and the hysteresis areas obtained from $F2.5_{4PG\text{-}IVM}$ and $F5_{4PG\text{-}IVM}$ were 725 and 2611 $Pa{\cdot}s^{-1}$, respectively. On the other hand, $F5_{10GL\text{-}IVM}$ and $F5_{2.5GL\text{-}IVM}$ also showed higher sprayed

areas (Table 4), but the hysteresis area was lower than those in $F2.5_{4PG\text{-}IVM}$ and $F5_{4PG\text{-}IVM}$. The yield value obtained in the rheograms for $F2.5_{4PG\text{-}IVM}$ and $F5_{4PG\text{-}IVM}$ were 3.29 and 13.8 Pa, respectively. Thus, further experiments were conducted with $F2.5_{4PG\text{-}IVM}$ and $F5_{4PG\text{-}IVM}$.

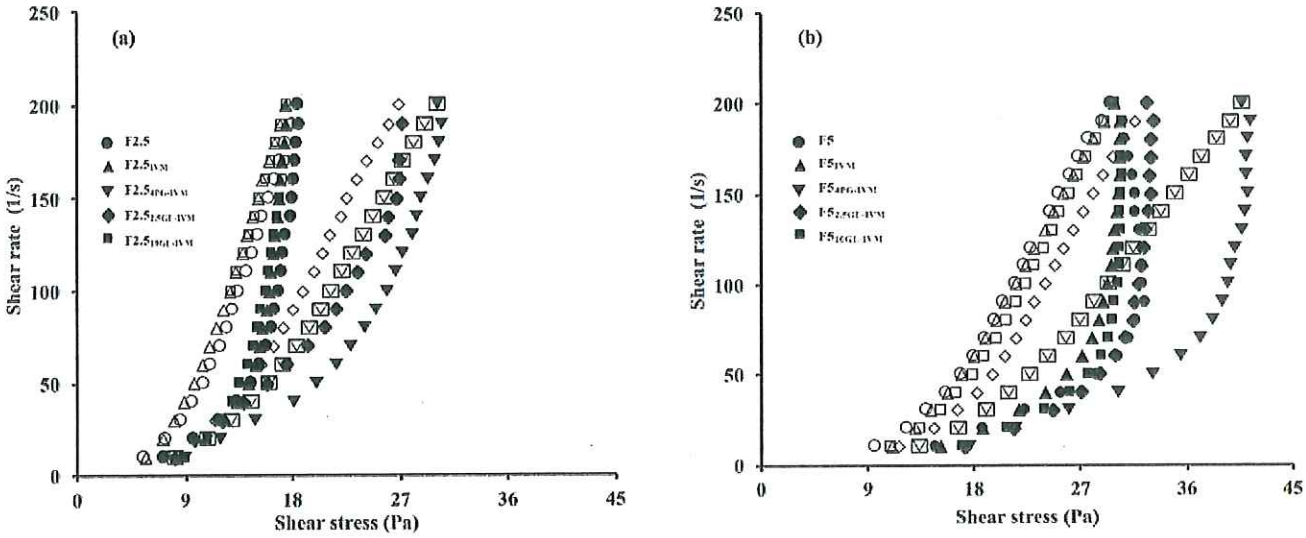

Fig. 6. Rheograms of several gel formulations at Pal-GH concentration of 2.5% (a) and 5% (b). Closed and open symbols indicate increasing and decreasing shear rate, respectively. Thixotropic behavior was clearly observed in all formulations. Symbols; ○ and ●: F2.5 (in Fig. 5a) or F5.0 (in Fig. 5b), △ and ▲: $F2.5_{IVM}$ (in Fig. 5a) or $F5.0_{IVM}$ (in Fig. 5b), ▽and ▼: $F2.5_{4PG\text{-}IVM}$ (in Fig. 5a) or $F5_{4PG\text{-}IVM}$ (in Fig. 5b), ◇ and ◆: $F2.5_{2.5GL\text{-}IVM}$ (in Fig. 5a) or $F5_{2.5GL\text{-}IVM}$ (in Fig. 5b), □ and ■: $F2.5_{10GL\text{-}IVM}$ (in Fig. 5a) or $F5_{10GL\text{-}IVM}$ (in Fig. 5b).

1.3.3. *In vitro* release of IVM from Pal-GH formulations

Because IVM is a highly lipophilic compound, soybean oil was used as a receiver medium in the *in vitro* release studies of IVM from formulations. The cumulative percentage

of IVM released from $F2.5_{4PG\text{-}IVM}$ and $F5_{4PG\text{-}IVM}$ was about 4.9% and 5.7% over 24 h, respectively (no significant differences were observed among all the tested Pal-GH formulations), whereas a released value of 13.6% was observed from the PG solution (Fig. 7).

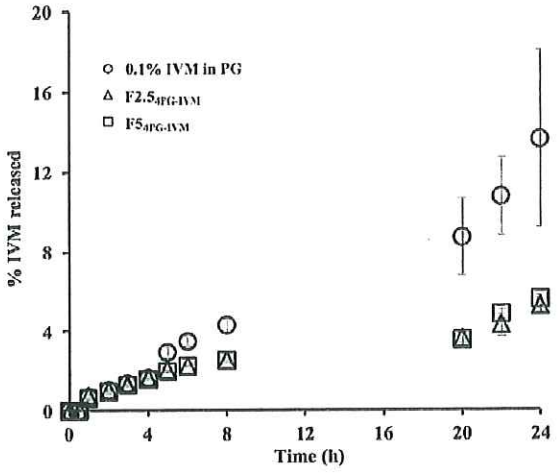

Fig. 7. IVM release profile from Pal-GH formulations. Significant differences were not observed between Pal-GH formulations but were observed with between control and Pal-GH formulations (*: $p<0.05$). Symbols; ○: 0.1% IVM in PG (control), △: $F2.5_{4PG\text{-}IVM}$, □: $F5_{4PG\text{-}IVM}$.

1.3.4. Skin disposition of IVM after topical application of Pal-GH formulations

Fig. 8 shows the skin concentration of IVM 24 h after topical application of $F2.5_{4PG\text{-}IVM}$ and $F5_{4PG\text{-}IVM}$ onto hairless rat skin. PG solution containing 0.1% IVM was used for comparison. The IVM concentration in the VED and stratum corneum was also investigated. A markedly higher IVM concentration in the stratum corneum was observed in all topically applied

formulations compared with the effective concentration reported by Haas *et al.* (2002) (40–80 ng/g). The IVM concentration in the stratum corneum that obtained from 0.1% IVM in PG was much higher than those with $F2.5_{4PG\text{-}IVM}$ and $F5_{4PG\text{-}IVM}$. However, the IVM concentrations in VED after topical application of $F2.5_{4PG\text{-}IVM}$ and $F5_{4PG\text{-}IVM}$ were significantly increased compared with that after topical application of 0.1% IVM in PG. Despite the IVM skin concentration observed with all formulations, no skin permeation of IVM was observed.

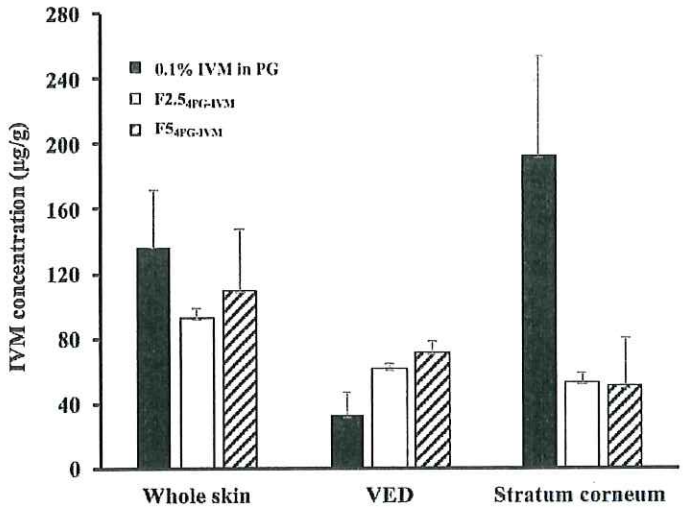

Fig. 8. IVM concentration in whole skin, VED and stratum corneum after topical application of Pal-GH gel formulations on hairless rat skin. The IVM concentration of the stratum corneum was estimated by dividing the IVM amount difference between the IVM amounts in the VED and whole skin by the weight of the stratum corneum. Significant differences were observed between Pal-GH formulations and 0.1% PG solution in the stratum corneum and VED (*: $p<0.05$). Closed columns: 0.1% IVM in PG, Open columns: $F2.5_{4GL\text{-}IVM}$, hatched columns: $F5_{4PG\text{-}IVM}$.

1.3.5. FT-IR measurement of $F2.5_{4PG\text{-}IVM}$ and pure IVM

FT-IR studies were carried out to investigate the interaction between IVM and Pal-GH (Fig. 9). The FT-IR spectra of IVM showed sharp peaks at: 3458.4 cm^{-1} due to axial deformation of free O-H; 2964.6 cm^{-1} characteristic of methyl groups; 2937.6 indicating axial deformation of C-H; 1730.1 cm^{-1} characteristic of saturated aliphatic ketone C=O stretching; 1676.1 cm^{-1} relating to unsaturated lactones with a double bond adjacent to the -O- group, owing to the C=C group; 1599.0 and 1454.3 cm^{-1} relating to moderate absorption of ketones; and 1200–1000 cm^{-1} showing the aliphatic ethers due to the asymmetric axial deformation of C-O-C. On the other hand, spectral peaks derived from IVM were not detected in F2.5 and $F2.5_{4PG}$, only a peak derived from the OH group and vibration of the C=O moiety in the carboxylates (1600 cm^{-1}) were observed.

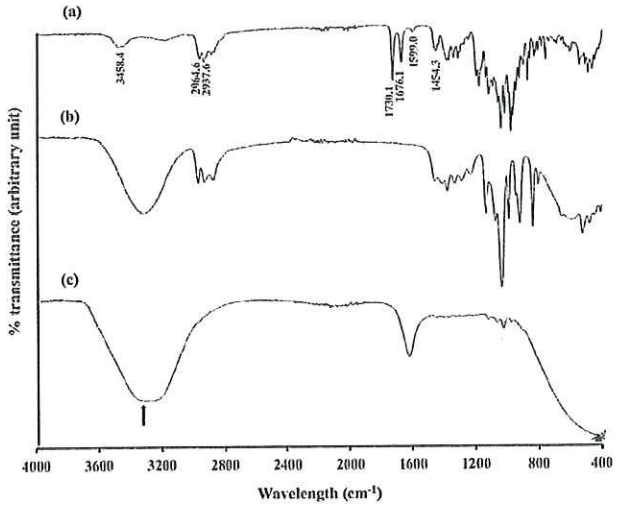

Fig. 9. FT-IR spectra of pure IVM (a), PG (b), and Pal-GH formulations (c).

1.4.Discussion

Pal-GH is a recently developed low molecular weight gelling agent. Matsumoto *et al.* reported its rheological properties, molecular assembled states, and the morphology of its network structure [24]. In the present study, we tried to develop a topically applicable GS formulation prototype using Pal-GH as a promising approach to increase IVM concentration in the skin of patients with scabies.

Topical drug application has many advantages, such as ease of administration and the ability to obtain high concentrations in the skin underneath the site of application, and reduced systemic side effects compared with oral administration or injection. Several reports have already revealed that topical application of IVM as a solution, lotion, or cream provided marketed improvement of scabies without serious side effects, although IVM concentration in the skin was not evaluated in these studies [25,26]. On the other hand, an IVM concentration of more than 400 ng/g skin tissue was observed after application of a bath formulation to rat skin. Haas *et al.* [10] reported that the IVM concentration in the stratum corneum ranged from 40 to 80 ng/g in patients with scabies, who responded to oral administration of IVM at a dose of 12 mg, and this is regarded as an effective dose.

In the present study, IVM application with a GS formulation ($F2.5_{4PG\text{-}IVM}$ and $F5_{4PG\text{-}IVM}$) showed much higher skin tissue concentration, more than 40 μg/g in the stratum corneum and VED, respectively (Fig. 8), although no skin permeation was observed due to its high

lipophilicity. Thus, a sufficient concentration was obtained for scabies treatment by application of Pal-GH formulations containing IVM. Because the skin concentration of drugs is generally related to their applied concentration (dose), adequate therapeutic skin concentration of IVM could be obtained by decreasing the applied concentration or dose in the formulation. The IVM concentration in VED obtained from the topical application of Pal-GH formulations was significantly ($p<0.05$) higher than that obtained from the topical application of 0.1% IVM in PG, although 0.1% IVM in PG showed a significantly ($p<0.05$) higher concentration in the stratum corneum compared with Pal-GH formulations. Because the complete removal of topically applied formulations from the skin surface is difficult, the IVM concentration in the stratum corneum might be overestimated, especially for the PG alone formulation, even after performing 20 washes to remove the formulation.

In addition, a GS formulation is useful to prevent scabies infection by direct skin contact, and it can be maintained at the site of application on skin by its thixotropic properties derived from the molecular interactions of Pal-GH via non-covalent bonding [27]. The obtained hysteresis loop showed that structural change was obtained using externally applied force on the formulations. The drawn rheograms differed according to the additives in the formulation (Fig. 6), because the thixotropic properties were influenced by several factors, and one of them was by mixing with additives [28]. Furthermore, the flow-ability of sprayed $F2.5_{4PG\text{-}IVM}$ and $F5_{4PG\text{-}IVM}$ was investigated to confirm the usefulness of the presently prepared gel spray

formulation. No flowing-down of sprayed $F2.5_{4PG\text{-}IVM}$ and $F5_{4PG\text{-}IVM}$ was observed on the vertical glass plate (data not shown). This finding showed that our formulations were suitable to maintain the sprayed area with easy spraying.

A marked interaction between IVM and Pal-GH could not be found using the FT-IR determination (Fig. 9) because of the low concentration of IVM in this formulation. In addition, IVM release from the prepared Pal-GH formulation was not changed by an increase in Pal-GH concentration. However, thixotropic behavior was changed by increasing Pal-GH concentration as well as the addition of additives in the formulation. This result suggested that microstructural changes in the Pal-GH formulation might be obtained by the additives in the formulation.

The mechanism of the enhancement effect on the skin concentration of IVM from Pal-GH formulations is not fully understood. The drug release rate and its subsequent skin permeation are linearly related to the thermodynamic activity in the formulation [29-31]. Thus, differences in the thermodynamic activity of the formulation might be a reason for the higher IVM concentration after application of the Pal-GH formulations. Since Pal GH has hydrophilic and lipophilic site, it can solubilize IVM, thereby affecting the thermodynamic activity of IVM. Increase in drug solubility in the formulation will lower its thermodynamic activity. Hence, decreases drug permeation through the skin. The partition and diffusion properties are affected by the thermodynamic activity and the physical state (solution/suspension) of IVM, as well as

the barrier function of the skin. Moreover, freely existing Pal-GH molecules might work as a penetration enhancer for IVM penetration into the skin.

Further efforts are needed to develop Pal-GH formulations and assess the therapeutic efficiency of our formulations. The present findings strongly suggested that the Pal-GH gel spray formulation (*i.e.*, $F2.5_{4PG\text{-}IVM}$, $F5_{4PG\text{-}IVM}$) developed here can be utilized as a promising new topical formulation for the treatment of scabies.

1.5. Chapter conclusion

The present data clearly indicated that application of Pal-GH gel formulations ($F2.5_{4PG\text{-}IVM}$ and $F5_{4PG\text{-}IVM}$) is a promising topical spray formulation. This approach may contribute to develop a new pharmaceutical additives, as a good formulation base for transdermal drug delivery and to enhance the skin concentration of mal-absorptive drugs from topical formulations. Further studies should be performed to clarify the mechanism of skin-penetration enhancement of drugs using Pal-GH formulations.

Chapter 2.

Combined use of *N*-palmitoyl-glycyl-histidine gel and several penetration enhancers on the skin permeation and concentration of metronidazole

2.1. Introduction

Low molecular weight gelators have been considered attractive novel soft materials over the past two decades. One such material, *N*-palmitoyl-glycyl-histidine (Pal-GH) was developed by Nissan Chemical Industries (Tokyo, Japan) and exhibits thixotropic behavior and high dissolving properties for a wide range of hydrophilic to lipophilic drugs. We reported on the usefulness of Pal-GH gel as a spray gel topical formulation base for the application of ivermectin (IVM) as lipophilic model drug [2]. An effective IVM concentration in the skin (more than 40 to 80 ng/g) was observed following the topical application. In addition, the Pal-GH GS formulations showed high spread-ability and low flow-ability on the applied skin site, suggesting that they may be a good formulation base for transdermal drug delivery.

Although skin is broadly utilized as an application site for many drugs with expected topical and systemic pharmacological effects, the uppermost skin layer, the stratum corneum, has a high barrier property against skin permeation by drugs. Thus, it is a formidable challenge to enhance the skin permeation of poorly skin-penetrating drugs such as water-soluble drugs [3,32].

The use of chemical penetration enhancers (CPEs) has been extensively studied in the last three to four decades [12] to achieve suitable skin permeation and/or local concentration of topically applied drugs. Many types of CPEs, such as alcohols, fatty acid esters, ether alcohols, and sulfoxides, have been evaluated mainly by *in vitro* skin permeation experiments. However, the skin permeation of Pal-GH gel and the combination of several CPEs has not been studied. In the present study, metronidazole (Fig. 10), (MTZ, molecular weight; 171.15 g/mol, logKo/w; −0.15), a hydrophilic drug with low skin permeability, was selected as the model drug, and propylene glycol (PG) [33-36], ethanol (EtOH) [37], isopropyl myristate (IPM) [38], diethylene glycol monoethyl ether (Transcutol®, TRANS) [39], and dimethyl sulfoxide (DMSO) [40] were selected as CPEs to represent alcohols, fatty acid esters, ether alcohols, and sulfoxides, respectively. DMSO can increase the lipid fluidity and promote drug partition [40–45]. PG [46–48] is known to solubilize α-keratin in the corneocytes, which is related to the intercellular penetration of drugs [49,50]. IPM directly acts on the stratum corneum, permeates into the lipid bilayer, and increases the fluidity of membranes [38,51]. Transcutol® is a powerful solubilizing agent and an attractive penetration enhancer due to its nontoxicity. EtOH extracts lipids to increase the lipid fluidity, enhances drug solubility in stratum corneum lipids, causes changes in skin hydration and alterations in keratinized proteins, and has a drug solvent effect. The skin concentration of MTZ was also evaluated, as it is closely related to the pharmacological and/or toxicological effects of MTZ.

Further studies would be needed to fully understand the detailed mechanism for the correlation between change in network structures of molecules with physical properties (thixotropic behavior), enhancement of skin permeation and concentration of hydrophilic and lipophilic drugs by Pal-GH gels. Finally, the author studied on a microscopic level of the fibrous structures and morphologies of Pal-GH gels, to confirm the changes of microstructural in the Pal-GH assembly upon addition of some enhancers. Morphological properties and microstructural of Pal-GH gels were also observed by light microscopy and TEM in this chapter.

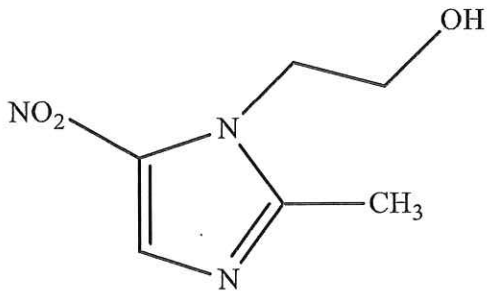

Fig. 10. Chemical structure of metronidazole

2.2. Materials and methods

2.2.1. Materials

Pal-GH premix (composed of 6% Pal-GH, 30% 1,2-octanediol, 20% 1,3-butanediol, 2% polyoxyethylene lauryl ether, 1% stearic acid, and 41% purified water) and propylene glycol alginate (PGA) were obtained from Nissan Chemical Industries, Ltd. (Tokyo, Japan).

MTZ was purchased from Tokyo Chemical Industry (Tokyo, Japan). PG was purchased from Kanto Chemical Co. Inc. (Tokyo, Japan). EtOH, TRANS, DMSO, and IPM were purchased from Wako Pure Chemicals Industries, Ltd. (Osaka, Japan). Other chemicals and reagents were of special grade or HPLC grade, purchased from Wako Pure Chemical Industries, Ltd. (Osaka, Japan), and were used without further purification.

2.2.2. Animal

Male hairless rats (WBM/ILA-Ht, 8 weeks of age, body weight of 200–250 g) were obtained from the Life Science Research Center, Josai University (Sakado, Saitama, Japan) or Ishikawa Experiment Animal Laboratories (Fukaya, Saitama, Japan). The animals were housed in temperature-controlled rooms (25 ± 2°C) with a 12 h light-dark cycle (7:00–19:00 h). The rats were allowed free access to food (Oriental Yeast Co., Tokyo, Japan) and tap water. All animal feeding and breeding procedures, and the experiments themselves were approved by the Institutional Animal Care and Use Committee of Josai University (April 6, 2017) with approval number H29003.

2.2.3. Preparation of applied formulations

Table 5 shows the compositions of the Pal-GH formulations and MTZ solution with or without a chemical enhancer. The Pal-GH formulations were prepared by a heating-and-

cooling method as follows: Pal-GH premix was stirred with a stirrer bar on a magnetic stirrer (RSH-IDN, AS ONE Corporation, Osaka, Japan) in purified water and maintained at 85 °C until completely dissolved. Then, MTZ (100 mg) was dissolved in the Pal-GH solution at 75 °C, followed by the addition of several CPEs (IPM, PG, DMSO, EtOH, and Transcutol®).

Table 5. Composition of the *N*-Palmitoyl-Glycine-Histidine (Pal-GH) gel formulations and metronidazole (MTZ) solution with or without a chemical enhancer prepared in this experiment. IPM = isopropyl myristate; PG = propylene glycol; ethanol; DMSO = dimethyl sulfoxide; and TRANS = Transcutol®.

Formulation Code	Pal-GH Conc. (Premix)	Chemical Penetration Enhancer
$F2.5_{MTZ}$	2.5%	No enhancer
$F5_{MTZ}$	5%	No enhancer
$F5_{IPM\text{-}MTZ}$		IPM 10%
$F5_{PG\text{-}MTZ}$		Propylene glycol 4%
$F5_{DMSO\text{-}MTZ}$		DMSO 5%
$F5_{EtOH\text{-}MTZ}$		Ethanol 20%
$F5_{TRANS\text{-}MTZ}$		isopropyl myristate 10%
$F10_{MTZ}$	10%	No enhancer
Aqueous solution		No enhancer
IPM_{MTZ}		IPM 10%
PG_{MTZ}		Propylene glycol 4%
$DMSO_{MTZ}$		DMSO 5%
$EtOH_{MTZ}$		Ethanol 20%
$TRANS_{MTZ}$		Transcutol 10%

Furthermore, a PGA aqueous solution was prepared by stirring in purified water at 85 °C for 1 h. The obtained Pal-GH solution was mixed with the PGA solution at 1000 rpm and 75 °C for 1 h (until homogenous). The Pal-GH gel formulation was kept at room temperature prior to use. Pal-GH gel formulations without CPE were also prepared. In addition to the Pal-

GH formulation, 1% MTZ solutions with and without CPE were also prepared to investigate the skin penetration enhancement effects from an aqueous solution. MTZ was completely dissolved in purified water and then CPE was added to the solution. The concentration of CPE in the MTZ solution was the same as that in the Pal-GH formulation.

2.2.4. *In vitro* skin permeation experiment

Full thickness hairless rat skin was excised from previously-shaved abdomens under intraperitoneally-administered anesthesia (medetomidine, 0.375 mg/kg; butorphanol, 2.5 mg/kg; and midazolam, 2 mg/kg). The excess fat was trimmed off and the skin was set in a Franz diffusion cell (effective diffusion area: 1.77 cm^2) with the epidermis side facing the donor cell (Fig. 11). The receiver cell was filled with 6.0 mL of phosphate buffered saline (PBS, pH 7.4), and 1 mL of PBS was applied to the epidermis side to reach an equilibration state for about 1 h. After an hour, the PBS of the epidermis side was replaced with the same volume of donor (1.0 mL of 1% MTZ solution or Pal-GH formulation) to commence the permeation experiment. The temperature was maintained at 32 °C for 24 h. At predetermined times, an aliquot (0.5 mL) was withdrawn from the receiver chamber, and the same volume of fresh PBS was added to keep the volume constant. The obtained sample was used to measure the MTZ concentration by HPLC.

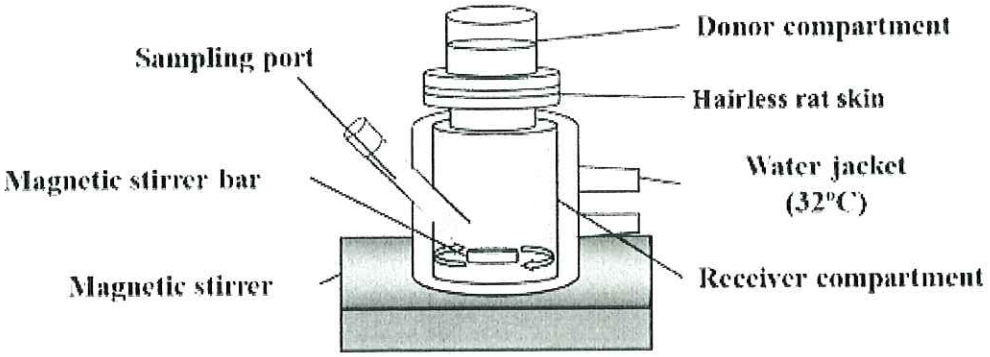

Fig. 11. Set-up of vertical type diffusion cell for *in vitro* permeation experiment

A side-by-side two-chamber diffusion cell with an effective permeation area of 0.95 cm^2 was used for the application of the MTZ solution containing IPM due to the low solubility of IPM in the aqueous solution. The MTZ solution containing the IPM suspension (3.0 mL) was applied to the epidermal side, and the same volume of PBS was applied to the dermal side. Each solution was constantly stirred throughout the experiment to maintain the homogeneity of the donor solution (IPM in water) with a stirrer bar and kept at 32 °C by water circulation in a chamber jacket. At predetermined times, an aliquot (0.5 mL) was withdrawn from the dermal side, and the same volume of fresh PBS was added to keep the volume constant. In vitro skin permeation parameter (flux, permeability coefficient, and lag time) were calculated from the slope of the steady state portion of the amount of permeated drug.

2.2.5. *In vitro* release experiment

The MTZ release over 6 h was evaluated from the Pal-GH gel formulations ($F2.5_{MTZ}$, $F5_{MTZ}$, $F10_{MTZ}$) and Pal-GH formulations containing CPEs. A dialysis membrane (molecular weight cut-off; 2000–14,000 Da, Sanko Junyaku Co., Tokyo, Japan) was soaked in PBS before being set in a vertical-type diffusion cell (effective diffusion area 0.95 cm^2), and the receiver chamber was maintained at 32 °C. The receiver cell was filled with 6 mL of PBS, and 1.0 mL of Pal-GH formulation was applied to the donor cell while the receiver solution was agitated at 500 rpm using a magnetic stirrer. An aliquot (0.5 mL) was withdrawn from the receiver chamber, and the same volume of PBS was added to the chamber to keep the volume constant. The amount of MTZ released was determined. The release rate was calculated with the Higuchi equation.

2.2.6. Evaluation of Rheological Properties for N-Palmitoyl-Glycine-Histidine (Pal-GH) Formulations

The rheological properties of the Pal-GH formulations were evaluated using a rotational viscometer (RE-215H, Toki Sangyo Co., Ltd., Tokyo, Japan). The rotation speed was increased from 0 to 100 rpm over 7.5 min and decreased from 100 to 0 rpm over an equal time period, and the temperature was maintained at 32 °C. The corn rotor was 3° × R14, sample volume was 0.4 mL, and a flow analysis method was used. The hysteresis loop, thixotropic index, and yield value of the Pal-GH gel formulations were evaluated. The hysteresis area and yield value

were calculated using VA 2000 software (Toki Sangyo Co., Ltd., Tokyo, Japan), whereas the thixotropic index was calculated by dividing the viscosity at 10 rpm by the viscosity at 100 rpm from the upward curve.

2.2.7. Skin concentration of MTZ

The skin concentrations of MTZ were evaluated after the application of selected Pal-GH formulations. At the end of the skin permeation experiment, the donor solution was removed using a cotton swab, and the skin sample was washed 10 times on the epidermis side and three times on the dermis side with 1 mL of PBS. The skin was blotted dry with Kimwipes® paper. The compound-applied area was cut out and divided into parts for full thickness and viable epidermis and dermis (VED). For the measurement of the MTZ concentration in VED, the stratum corneum was removed by tape-stripping 20 times from the full-thickness skin using an adhesive tape (Cellotape®, Nichiban, Tokyo, Japan).

The MTZ concentrations in the full-thickness skin as well as VED were determined, and the amount of MTZ in the stratum corneum was calculated by subtracting the amount in the VED from that in the full-thickness skin. Then, the MTZ concentration in the stratum corneum was estimated under the assumption that the density and the thickness of the stratum corneum would be 1.2 g/cm^3 [23] and 15.4 μm, respectively. The obtained skin piece (0.05 g) was reduced in size using scissors and homogenized at 12,000 rpm (4 °C, 5 min) with 0.45 mL

of methanol for 2.5 min using a homogenizer (Polytron PT-MR 3000; Kinematica Inc., Littaue-Lucerne, Switzerland). Methanol (0.5 mL) was added and homogenized again for 2.5 min, followed by agitation at 32 °C for 15 min. Then, the mixture was centrifuged at 5000 rpm (4 °C, 5 min). The supernatant (100 μL) was mixed with the same volume of methanol and then agitated and centrifuged again under the same conditions. Finally, the obtained sample was used to detect the MTZ concentration by HPLC.

2.2.8. Determination of MTZ

The obtained supernatant (20 μL) was injected into an HPLC system and measured under the following conditions.

The HPLC system (Shimadzu, Kyoto, Japan) consisted of a system controller (CBM-20A), pump (LC-20AD), degasser (DGU-20A3), auto-injector (SIL-20AC), a column oven (CTO-20A), UV detector (SPD-M20A), and analysis software (LC Solution). The column was a Superiorex® ODS (5 μm, 4.6 × 250 mm) (Shiseido, Fine Chemicals; Tokyo, Japan), which was maintained at 40 °C. The mobile phase was methanol : water = 4 : 6 v/v (0–7 min). The flow rate was adjusted to 1.0 mL/min. The MTZ was detected at UV 254 nm. Briefly, the receiving solutions were mixed with the same volume of methanol and vortexed. After centrifugation at 21,500× g at 4 °C for 5 min, the resulting supernatant (20 μL) was injected directly into the HPLC system.

2.2.9. Small angle X-ray analysis

X-ray diffraction analyses were performed with a small-angle X-ray diffraction system (Nano-Viewer, Rigaku Corporation, Tokyo, Japan), which was equipped with an X-ray generator (CuKα radiation, λ = 1.5418 Å), at a scanning rate of 5°. Diffraction analyses were performed using a vacuum-resistant glass capillary cell at 25 °C for 1 h. The scattering intensity was normalized by the decayed direct beam intensity.

2.2.10. Digital microscopy

Table 6 shows the measurement conditions using the electron microscope.

Table 6. Observation condition of electron microscopy

Apparatus	VHX-5000	
Brightness	Shutter speed	Auto 70
	Gain	Auto 50
Lighting	Epi-illumination	On 255
		Ring lighting
	Transmitted lighting	On 255
Image quality UP HDR	Adjust brightness	21
	Texture enhancement	30
	Contrast	18
	Color adjustment	58

Pal-GH gel formulation was pre-warmed at 75 °C, then 10 μL of each prepared formulation was dropped in a glass bottom dish and sealed with a glass cover, then a wight of 930 g was placed on it to confirm the same pressure to each sample. The sample was left

undisturbed for 1 min to equilibrate at room temperature prior to observation using an electron digital microscopy (VHX-5000, KEYENCE, Osaka, Japan).

2.2.11. Transmission electron microscopy (TEM)

A hydrogel sample was diluted 20 times with purified water and placed on a carbon-coated copper grid (400-Cu grids). Then, the samples were stained with 2% uranyl acetate. TEM images were recorded by a JEM-1200 (JEOL, Tokyo, Japan). The observations were carried out at an acceleration voltage of 80 kV. The observations were performed at Hanaichi Ultrastructure Research Institute (Okazaki, Aichi, Japan).

2.2.12. Statistical analysis

Statistical analyses of the *in vitro* skin permeation, release, and skin concentration of MTZ were performed using one-way ANOVA and Tukey's Honestly Significant Different (HSD) post hoc analyses, and p-values less than 0.05 were considered to be significant.

2.3. Results

2.3.1. Physical properties of Pal-GH gel formulation

Fig. 12 shows the state of the Pal-GH gel formulation in the bottles. The bottles were put in an inverse direction immediately (Fig. 12a) and after 5 min (Fig. 12b) of being shaken

at room temperature were tapped 10 times. $F2.5_{MTZ}$, $F5_{MTZ}$, and $F10_{MTZ}$ are shown from left to right in both Fig. 12 a, b. These formulations showed a sol-gel transition within 5 min.

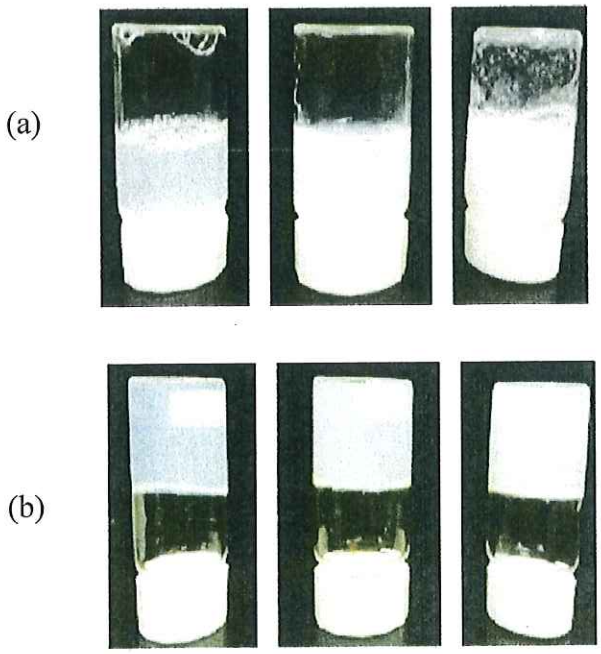

Fig. 12. Photographs of the state of the N-Palmitoyl-Glycine-Histidine (Pal-GH) gel formulation in the bottles. The bottles were placed in an inverse position immediately (a) and 5 min after (b) shaking. The Pal-GH concentrations are, from left to right in both photos, 2.5, 5, and 10%.

2.3.2. *In vitro* skin permeation of MTZ from aqueous solution

Fig. 13 shows the permeation profiles of MTZ through excised hairless rat skin from the aqueous solution with or without CPE. The MTZ solution without CPE was used as a control. Only IPM_{MTZ} was associated with a skin penetration enhancement effect when

compared with the control, and no skin penetration enhancement effects were observed in the other CPEs. PG_{MTZ} exhibited a similar MTZ permeation profile to the control, whereas $TRANS_{MTZ}$ and $EtOH_{MTZ}$ showed dramatically decreased permeation profiles when compared with the control.

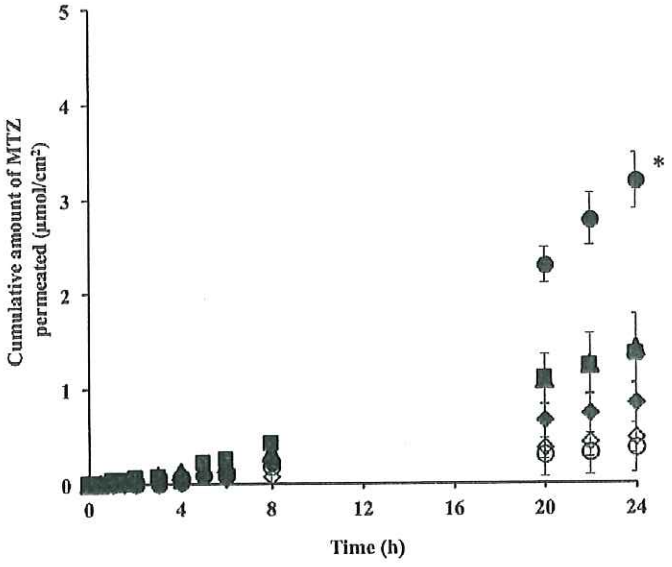

Fig. 13. Permeation profiles of metronidazole (MTZ) through the excised hairless rat skin from its aqueous solution with or without a chemical enhancer. MTZ permeation was significantly (* $p < 0.05$) improved by IPM when compared with the aqueous solution without an enhancer (control) and other chemical penetration enhancers (CPEs). Symbols: ▲: aqueous solution, ●: IPM_{MTZ}, ■: propylene glycol (PG_{MTZ}), ◆: dimethyl sulfoxide ($DMSO_{MTZ}$), ◇: ethanol ($EtOH_{MTZ}$), ○: $TRANS_{MTZ}$.

2.3.3. *In Vitro* release and skin permeation of MTZ from Pal-GH gels

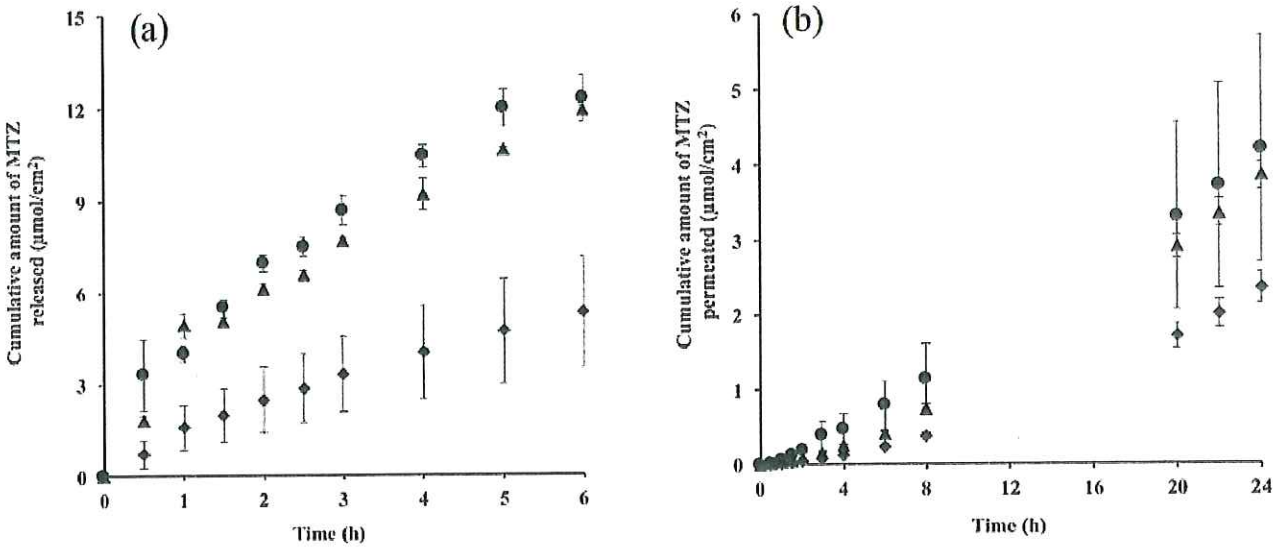

Fig. 14. *In vitro* release (a) and skin permeation (b) of MTZ from different concentrations of Pal-GH gels. Symbols: ●: F2.5$_{MTZ}$, ▲: F5$_{MTZ}$, ◆: F10$_{MTZ}$ (mean ± S.E., n = 4).

Fig. 14a shows the MTZ release profiles following exposure to different concentrations of Pal-GH gel formulation. The levels of MTZ release from F2.5$_{MTZ}$ and F5$_{MTZ}$ were similar, whereas that from F10$_{MTZ}$ was lower

Fig. 14b shows the effect of the Pal-GH concentration on the time course of the cumulative amount of MTZ permeation through hairless rat skin after application of Pal-GH gel formulations. The cumulative levels of MTZ permeation over 24 h from F2.5$_{MTZ}$ (Q_{24h}; 4.2 μmol/cm^2) and F5$_{MTZ}$ (Q_{24h}; 3.8 μmol/cm^2) were higher than that from F10$_{MTZ}$ (Q_{24h}; 2.4

μmol/cm2). $F2.5_{MTZ}$ showed a large coefficient of variation (CV) (>0.7) for all sampling points, whereas $F5_{MTZ}$ and $F10_{MTZ}$ had CVs < 0.3 for all sampling points. Thus, the $F5_{MTZ}$ formulation was used to evaluate the effect of CPEs on the skin permeation of MTZ.

Furthermore, when the amounts of the MTZ releases were plotted against the squared root of time, straight lines were observed regardless of the Pal-GH concentration (Fig. 14c). MTZ release from $F2.5_{MTZ}$, $F5_{MTZ}$, and $F10_{MTZ}$ can be explained by the Higuchi equation, suggesting that the drug was homogenously distributed in the gel

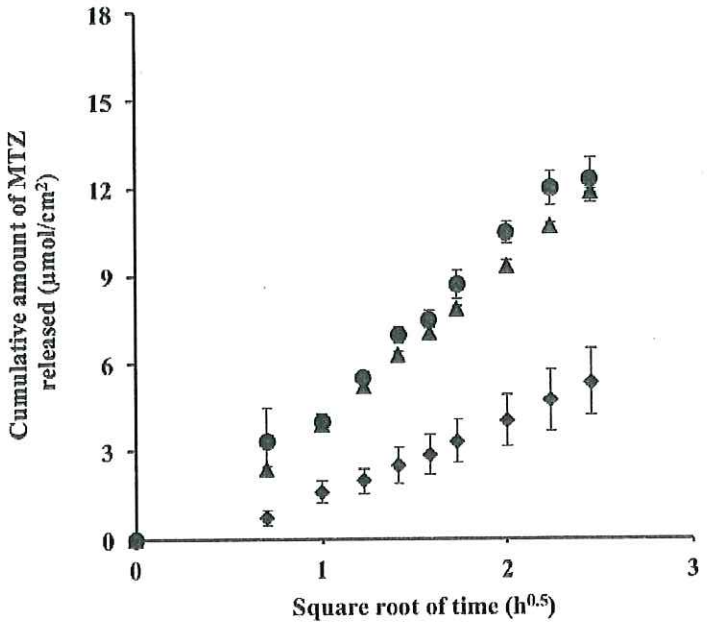

Fig. 14c. Higuchi plot analysis of the *in vitro* release of MTZ from different concentrations of Pal-GH gels. Symbols: ●: $F2.5_{MTZ}$, ▲: $F5_{MTZ}$, ◆: $F10_{MTZ}$ (Mean ± S.E., $n = 4$).

$F5_{MTZ}$, $F5_{IPM\text{-}MTZ}$, and $F5_{PG\text{-}MTZ}$ showed higher release rates than those from other formulations (Table 7). Significant differences in release rates were observed between all formulations except between $F5_{MTZ}$ and $F5_{IPM\text{-}MTZ}$ ($p < 0.05$) (Table 6).

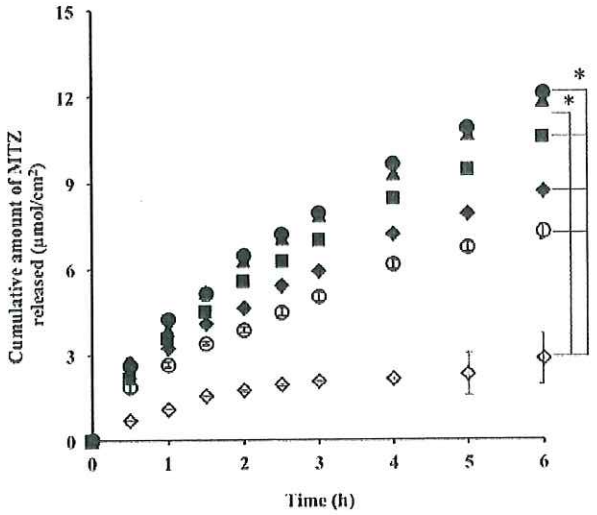

Fig. 15. The effect of CPEs in Pal-GH gel formulations on the MTZ release profiles. Symbols: ■: $F5_{PG\text{-}MTZ}$, ●: $F5_{IPM\text{-}MTZ}$, ▲: $F5_{MTZ}$, ◆: $F5_{DMSO\text{-}MTZ}$, ◇: $F5_{EtOH\text{-}MTZ}$, ○: $F5_{TRANS\text{-}MTZ}$ (Mean ± S.E., $n = 3$–4).

Significant differences in MTZ release were observed among all formulations except between $F5_{MTZ}$ and $F5_{IPM\text{-}MTZ}$ (* $p < 0.05$),

Table 6. Release rates of Pal-GH gel formulations.

Formulation Code	Release Rate (K) ($\mu mol/cm^2/h^{0.5}$)
$F5_{MTZ}$	4.99 ± 0.99
$F5_{IPM\text{-}MTZ}$	5.07 ± 0.09
$F5_{PG\text{-}MTZ}$	4.43 ± 0.07
$F5_{DMSO\text{-}MTZ}$	3.53 ± 0.05
$F5_{EtOH\text{-}MTZ}$	1.11 ± 0.09
$F5_{TRANS\text{-}MTZ}$	3.06 ± 0.11

Significant differences in the release rates were observed between all formulations except between $F5_{MTZ}$ and $F5_{IPM\text{-}MTZ}$ ($p < 0.05$).

Fig. 15 shows the effects of the CPEs in the Pal-GH gel formulations on the MTZ release profile. Compared with $F5_{MTZ}$, $F5_{IPM\text{-}MTZ}$ and $F5_{PG\text{-}MTZ}$ had similar profiles, whereas $F5_{DMSO\text{-}MTZ}$, $F5_{EtOH\text{-}MT}$, and $F5_{TRANS\text{-}MTZ}$ had significantly ($p < 0.05$) lower release profiles.

Fig. 16 shows the effect of the CPEs in the Pal-GH gel formulations on the time course of cumulative skin permeation of MTZ. MTZ permeation from $F5_{IPM\text{-}MTZ}$ and $F5_{PG\text{-}MTZ}$ was improved compared to that of $F5_{MTZ}$ and commercial products. In contrast, the levels of MTZ permeation from $F5_{DMSO\text{-}MTZ}$, $F5_{EtOH\text{-}MT}$, and $F5_{TRANS\text{-}MTZ}$ were lower than that from $F5_{MTZ}$. However, $F5_{DMSO\text{-}MTZ}$ and $F5_{EtOH\text{-}MTZ}$ showed higher levels, and $F5_{TRANS\text{-}MTZ}$ exhibited a lower level of permeation compared to the aqueous solution (1% MTZ solution). Pal-GH gels showing higher levels of MTZ release ($F2.5_{MTZ} \cong F5_{MTZ} > F10_{MTZ}$) exhibited higher levels of skin permeation ($F2.5_{MTZ} \cong F5_{MTZ} > F10_{MTZ}$), as shown in Fig. 14a, but the release order from the Pal-GH gels containing CPEs did not match that obtained from the permeation results.

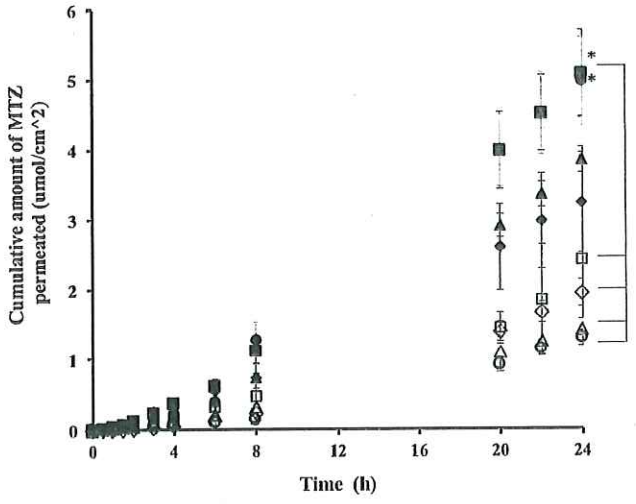

Fig. 16. The effect of CPEs in Pal-GH gel formulations on the skin permeation profiles. Significant differences in MTZ permeation between $F5_{PG\text{-}MTZ}$ and $F5_{EtOH\text{-}MTZ}$, $F5_{TRANS\text{-}MTZ}$, commercial product or solution MTZ; and between $F5_{IPM\text{-}MTZ}$ and $F5_{EtOH\text{-}MTZ}$, $F5_{TRANS\text{-}MTZ}$, commercial product or solution MTZ (* $p < 0.05$). Symbols: ■: $F5_{PG\text{-}MTZ}$, ●: $F5_{IPM\text{-}MTZ}$, ▲: $F5_{MTZ}$, ◆: $F5_{DMSO\text{-}MTZ}$, ◇: $F5_{EtOH\text{-}MTZ}$, ○: $F5_{TRANS\text{-}MTZ}$, Δ: Aqueous solution, : commercial product (Mean ± S.E., $n = 3$–4).

Table 8. Fluxes, permeability coefficients, and lag times of the Pal-GH gel formulations.

Formulation Code	Flux ($\mu g/cm^2/h$)	Permeability Coefficient ($\times 10^{-7}$ cm/s)	Lag Time (h)
$F5_{MTZ}$	17.7 ± 1.3	5.02 ± 0.37	1.59 ± 0.09
$F5_{IPM\text{-}MTZ}$ *,#	29.44 ± 7.5	8.43 ± 2.14	1.61 ± 023
$F5_{PG\text{-}MTZ}$ *,#	26.8 ± 4.79	7.69 ± 1.37	1.47 ± 0.21
$F5_{DMSO\text{-}MTZ}$	17.08 ± 4.73	4.82 ± 1.33	1.60 ± 0.44
$F5_{EtOH\text{-}MTZ}$	5.68 ± 1.01	1.59 ± 0.28	2.1 ± 0.23
$F5_{TRANS\text{-}MTZ}$	3.54 ± 0.79	0.99 ± 0.22	1.86 ± 0.2

Significant difference ($p < 0.05$) between $F5_{IPM\text{-}MTZ}$ and $F5_{TRANS\text{-}MTZ}$ or $F5_{EtOH\text{-}MTZ}$, $F5_{PG\text{-}MTZ}$, and $F5_{TRANS\text{-}MTZ}$ or $F5_{EtOH\text{-}MTZ}$ for flux (*) and permeability coefficients (#).

Table 8 summarizes the skin permeation fluxes, permeability coefficients, and lag times that were calculated from the skin permeation profiles of MTZ. $F5_{IPM\text{-}MTZ}$ and $F5_{PG\text{-}MTZ}$ showed higher fluxes and permeability coefficients compared with the other formulations. Significant differences in the fluxes and permeability coefficients were also observed between $F5_{IPM\text{-}MTZ}$ and $F5_{TRANS\text{-}MTZ}$ or $F5_{EtOH\text{-}MTZ}$ as well as between $F5_{PG\text{-}MTZ}$ with $F5_{TRANS\text{-}MTZ}$ or $F5_{EtOH\text{-}MTZ}$.

2.3.4. Skin disposition of MTZ after topical application of Pal-GH formulations

Figure 17 shows the skin concentration of MTZ after the *in vitro* skin permeation experiment had been completed (24 h). A topical application of 1% MTZ solution was tested for comparison (control). MTZ concentrations were increased throughout the skin samples in the following order: control, $F5_{MTZ}$, $F5_{PG\text{-}MTZ}$, and then $F5_{IPM\text{-}MTZ}$. This order was also observed in MTZ concentrations in both the stratum corneum and the VED. In addition, the enhancement ratios of the MTZ concentration in the skin as a whole after the application of $F5_{MTZ}$, $F5_{PG\text{-}MTZ}$, and $F5_{IPM\text{-}MTZ}$ were 7.2, 9.1, and 9.5-fold, respectively, versus that obtained from the control. $F5_{PG\text{-}MTZ}$ and $F5_{IPM\text{-}MTZ}$ had 1.2 and 1.3-fold higher concentrations, respectively, compared to $F5_{MTZ}$. In contrast, 30, 50, and 55-fold higher concentrations were obtained in the stratum

corneum after the application of $F5_{MTZ}$, $F5_{PG\text{-}MTZ}$, and $F5_{IPM\text{-}MTZ}$, respectively, compared to the control. $F5_{PG\text{-}MTZ}$ and $F5_{IPM\text{-}MTZ}$ had 1.6 and 1.8-fold higher concentrations, respectively, compared to $F5_{MTZ}$. Meanwhile, 1.8, 2.6, and 3.1-fold higher concentrations were achieved in the VED after the application of $F5_{MTZ}$, $F5_{PG\text{-}MTZ}$, and $F5_{IPM\text{-}MTZ}$, respectively, and 1.5 and 1.7-fold higher concentrations were obtained for $F5_{PG\text{-}MTZ}$ and $F5_{IPM\text{-}MTZ}$, respectively, compared to $F5_{MTZ}$.

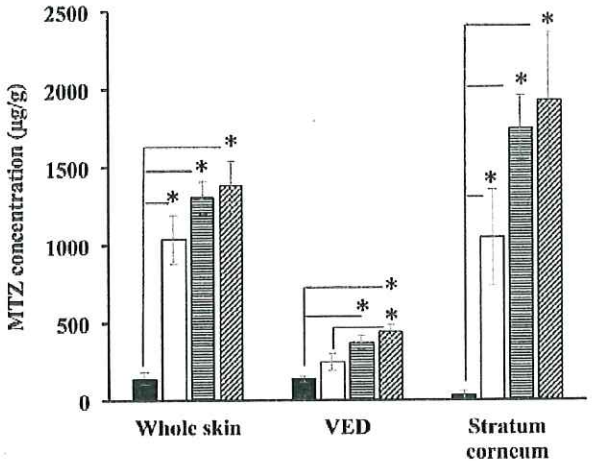

Fig. 17. MTZ concentrations in the skin as a whole, the viable epidermis and dermis (VED), and the stratum corneum after the topical application of Pal-GH gel formulations on hairless rat skin.

Significant differences were observed between $F5_{MTZ}$, $F5_{PG\text{-}MTZ}$, $F5_{IPM\text{-}MTZ}$, and 1% solution of MTZ in the whole skin, and stratum corneum (* $p < 0.05$). Additionally, significant differences were observed between $F5_{PG\text{-}MTZ}$ and $F5_{IPM\text{-}MTZ}$ with a 1% solution of MTZ and between $F5_{IPM\text{-}MTZ}$ with $F5_{MTZ}$ in the VED (* $p < 0.05$). The MTZ concentration in the stratum corneum was estimated by dividing the MTZ difference (between the VED and whole skin) by the weight of the stratum corneum. Closed columns: 1% MTZ solution, open columns: $F5_{MTZ}$, horizontal striped columns: $F5_{PG\text{-}MTZ}$, striped columns: $F5_{IPM\text{-}MTZ}$.

2.3.5. Thixotropic properties of Pal-GH gel formulations

The thixotropic properties of Pal-GH gel formulations were investigated. Table 9 and Figure 18 show the time-dependent viscosity changes of $F5_{MTZ}$, $F5_{PG\text{-}MTZ}$, $F5_{IPM\text{-}MTZ}$, $F5_{TRANS\text{-}}$

$_{MTZ}$, $F5_{EtOH-MTZ}$, and $F5_{DMSO-MTZ}$. The thixotropic behaviors changed by the addition of CPE to the formulation. In particular, the area of hysteresis loops of $F5_{PG-MTZ}$ (945 Pa/s), $F5_{IPM-MTZ}$ (1805 Pa/s), $F5_{TRANS-MTZ}$ (2102 Pa/s), $F5_{EtOH-MTZ}$ (2777 Pa/s), and $F5_{DMSO-MTZ}$ (1241 Pa/s) increased compared to that of $F5_{MTZ}$ (775 Pa/s). Thixotropic may also be expressed as the thixotropic index, which is the ratio of viscosities measured at speeds that have a ratio 1:10 rpm. The obtained thixotropic index values of $F5_{PG-MTZ}$ (5.57), $F5_{IPM-MTZ}$ (5.83), and $F5_{TRANS-MTZ}$ (5.35) were similar to that of F5MTZ (5.71), whereas the thixotropic index values of $F5_{EtOH-MTZ}$ (8.29) and $F5_{DMSO-MTZ}$ (7.1) were higher than that of $F5_{MTZ}$. In addition, the yield values of these formulations also changed, and the values for $F5_{PG-MTZ}$, $F5_{IPM-MTZ}$, $F5_{TRANS-MTZ}$, $F5_{EtOH-MTZ}$, and $F5_{DMSO-MTZ}$ increased to 11, 13, 13, 14, and 14 Pa, respectively, from the $F5_{MTZ}$ value of 8.0 Pa.

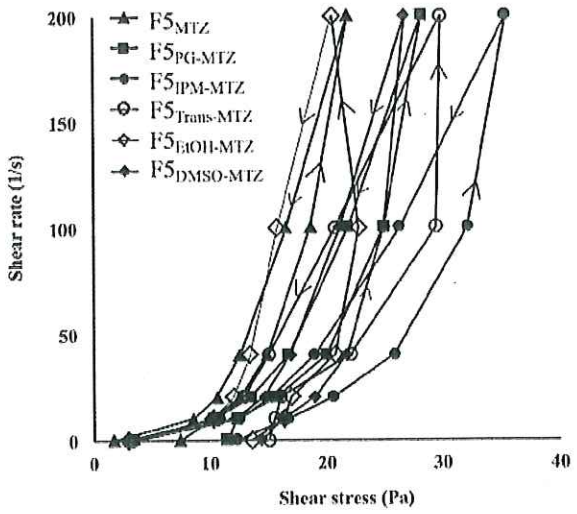

Fig. 18. Thixotropic properties of the Pal-GH gel formulations.

Table 9. Viscosities of the Pal-GH gel formulations.

	Viscosity (mPa.s)											
rpm	$F5_{-MTZ}$		$F5_{IPM-MTZ}$		$F5_{PG-MTZ}$		$F5_{DMSO-MTZ}$		$F5_{EtOH-MTZ}$		$F5_{TRANS-MTZ}$	
	upward	downward	upward	downward	upward	downward	upward	downward	upward	downward	upward	downward
0.01	$3.75x10^5$	$8.75x10^4$	$6.12x10^5$	$1.68x10^5$	$5.75x10^5$	$1.75x10^5$	$7.19x10^5$	$1.81x10^5$	$6.81x10^5$	$1.50x10^5$	$7.50x10^5$	$1.62x10^5$
5	$1.02x10^3$	$8.62x10^2$	$1.67x10^3$	$1.25x10^3$	$1.22x10^3$	$1.04x10^3$	$1.62x10^3$	$1.21x10^3$	$1.63x10^3$	$1.02x10^3$	$1.55x10^3$	$1.07x10^3$
10	$6.25x10^2$	$5.31x10^2$	$1.03x10^3$	$7.62x10^2$	$7.87x10^2$	$6.75x10^2$	$9.50x10^2$	$7.31x10^2$	$8.50x10^2$	$6.00x10^2$	$8.01x10^2$	$6.44x10^2$
20	$3.72x10^2$	$3.12x10^2$	$6.47x10^2$	$4.75x10^2$	$5.01x10^2$	$4.18x10^2$	$5.44x10^2$	$4.22x10^2$	$5.19x10^2$	$3.34x10^2$	$5.53x10^2$	$3.75x10^2$
50	$1.86x10^2$	$1.65x10^2$	$3.21x10^2$	$2.63x10^2$	$2.50x10^2$	$2.18x10^2$	$2.50x10^2$	$2.11x10^2$	$2.27x10^2$	$1.57x10^2$	$2.95x10^2$	$2.07x10^2$
100	$1.09x10^2$	$1.09x10^2$	$1.76x10^2$	$1.76x10^2$	$1.41x10^2$	$1.41x10^2$	$1.33x10^2$	$1.33x10^2$	$1.02x10^2$	$1.02x10^2$	$1.49x10^2$	$1.49x10^2$

2.3.7. Small angle X-ray analysis

Fig. 19 shows X-ray diffraction analysis. A broad scattering pattern of SAXS result was confirmed in the observation that micelle-like assemblies was formed.

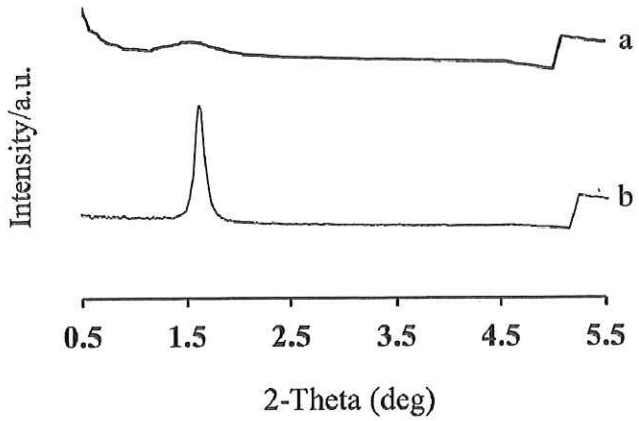

Fig. 19. SAXS profiles of Pal-GH containing MTZ (a) and Pal-GH (b).

Each curve is normalized and is horizontally shifted for clarity.

2.3.8. Microscopic observation of Pal-GH gels

Fig. 20 shows results by the light microscopic observation of Pal-GH gel formulations

to confirm the structure assembled by Pal-GH molecules. This experiment was conducted with Pal-GH formulations containing MTZ. A network structures were confirmed in all the formulations, except for IPM containing formulation. $F5_{IPM}$ showed lipid droplet-like structures in the formulation. The different mechanistic properties by the addition of IPM were not clearly understood. Then, Pal-GH gels were observed by TEM.

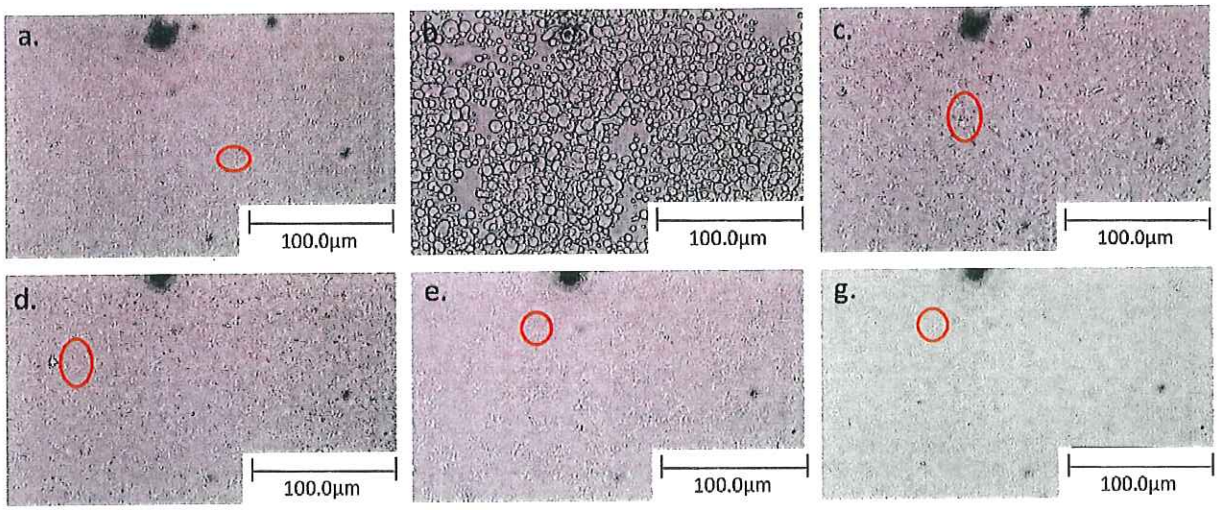

Fig. 20. Light microscopic observation of 5% Pal-GH gel formulation at magnification x1000 without (a) and with IPM, PG, DMSO, EtOH and Transcutol® in the formulations (b-f), respectively (red marks indicating fiber).

2.3.9. TEM Observation

The TEM observations were carried out to confirm the change in the Pal-GH assembly upon addition of several enhancers. TEM images of Pal-GH gel formulations; $F5_{MTZ}$, $F5_{EtOH}$-

$_{MTZ}$ and $F5_{TRANS\text{-}MTZ}$, showed homogeneous and straight fibrous structures, whereas fragmented fibrous structures were also observed in $F5_{EtOH\text{-}MTZ}$ and $F5_{TRANS\text{-}MTZ}$ (Fig. 21).

On the other hand, $F5_{IPM\text{-}MTZ}$, $F5_{PG\text{-}MTZ}$ and $F5_{DMSO\text{-}MTZ}$ had straight, but twisted fibrous. Table 10 is explanation of the TEM observation results.

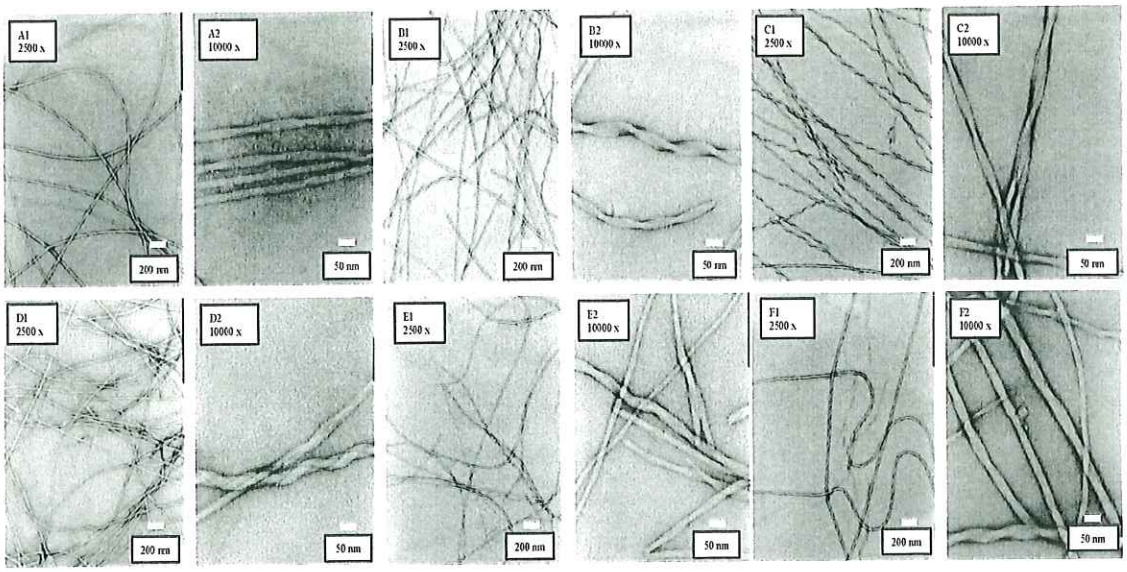

Fig. 21. TEM observation results of the Pal-GH gel formulations at different magnifications (x2500 and x10,000). $F5_{MTZ}$ (A1, A2), $F5_{IPM\text{-}MTZ}$ (B1, B2), $F5_{PG\text{-}MTZ}$ (C1, C2), $F5_{DMSO\text{-}MTZ}$ (D1, D2), $F5_{EtOH\text{-}MTZ}$ (E1, E2), and $F5_{TRANS\text{-}MTZ}$ (F1, F2).

Table 10. Description of TEM observation result

CPEs	Straight fiber	Twisted fiber	Fragmented shape	Highly dense fiber
$F5_{MTZ}$	○			○
$F5_{IPM\text{-}MTZ}$	○	○		○
$F5_{PG\text{-}MTZ}$	○	○		○
$F5_{DMSO\text{-}MTZ}$	○	○		○
$F5_{EtOH\text{-}MTZ}$	○		○	
$F5_{TRANS\text{-}MTZ}$	○		○	

2.4. Discussion

The skin permeation of MTZ was improved by the Pal-GH gel formulation. Supramolecular hydrogels with three-dimensional network structures can be formed through physical enlargement of nanofiber assemblies composed of amphiphilic molecules. Many published reports have shown that three-dimensional structures, such as micelles, lamella, and non-lamella, are useful drug carriers that can increase the skin permeation of entrapped drugs. A broad scattering SAXS pattern was confirmed for $F5_{MTZ}$ (Fig. 19). Generally, micelle-like assemblies that are formed by amphiphilic molecules show a broadening peak [24]. Thus, the micelle-like assemblies in Pal-GH gels may act as drug carriers and enhance the skin permeation of MTZ.

Interestingly, the skin permeation of MTZ from $F10_{MTZ}$ was lower than those from $F2.5_{MTZ}$ and $F5_{MTZ}$ (Fig. 14b). The drug release profile from $F10_{MTZ}$ was lower than those of $F2.5_{MTZ}$ and $F5_{MTZ}$ (Fig. 14a) because of the higher viscosity of $F10_{MTZ}$. Since the skin permeation of MTZ must be related to its release profile, the lower MTZ release may be a reason for lower MTZ permeation from $F10_{MTZ}$. MTZ release from $F2.5_{MTZ}$, $F5_{MTZ}$, and $F10_{MTZ}$ can be explained by the Higuchi equation, suggesting that the drug was homogenously distributed in the gel (Fig. 14c).

When compared to $F5_{MTZ}$, similar MTZ release profiles were observed in $F5_{IPM\text{-}MTZ}$ and $F5_{PG\text{-}MTZ}$ (Fig. 15). On the other hand, $F5_{EtOH\text{-}MTZ}$, $F5_{TRANS\text{-}MTZ}$, and $F5_{DMSO\text{-}MTZ}$ showed lower levels of MTZ release (Table 7). It would be reasonable to conclude that skin permeation profile and release of MTZ are related, each other as shown in Fig. 14. However, the MTZ release order from Pal-GH containing CPE did not correspond to its skin permeation order, suggesting that the effects of CPE on the skin barrier function might be associated with higher skin permeation of MTZ.

Among the CPEs, the IPM containing formulation, $F5_{IPM\text{-}MTZ}$, and the PG containing one, $F5_{PG\text{-}MTZ}$, showed higher levels of skin permeation of MTZ than $F5_{MTZ}$ (Fig. 16). These results support our finding that the permeability coefficients of $F5_{IPM\text{-}MTZ}$ and $F5_{PG\text{-}MTZ}$ were the highest (Table 8). Therefore, $F5_{IPM\text{-}MTZ}$ and $F5_{PG\text{-}MTZ}$ could increase the skin permeation of MTZ by increasing the drug partition into the stratum corneum from gel. On the other hand, no skin permeation enhancement was observed in the other CPEs containing Pal-GH formulations ($F5_{EtOH\text{-}MTZ}$, $F5_{TRANS\text{-}MTZ}$, and $F5_{DMSO\text{-}MTZ}$) when compared to $F5_{MTZ}$. Since the penetration enhancement effect from aqueous solution of MTZ with several enhancers (without Pal-GH) was only observed in 1% MTZ solution with IPM (IPM_{MTZ}) in the present study (Figure 13), it may be reasonable to conclude that $F5_{PG\text{-}MTZ}$ has a penetration enhancement effect. 1% MTZ solution with PG (PG_{MTZ}), 1% MTZ solution with DMSO ($DMSO_{MTZ}$), and 1% MTZ solution with ethanol ($EtOH_{MTZ}$) did not display this effect; however, the levels of

MTZ permeation from $F5_{PG\text{-}MTZ}$, $F5_{DMSO\text{-}MTZ}$, and $F5_{EtOH\text{-}MTZ}$ were 3.6, 2.3, and 1.3-fold higher than that of the control solution.

The Pal-GH gel had a fibrous structure in all formulations. Thus, the construction of fibrous micelle-like Pal-GH assemblies may be a reason for the increase in MTZ permeation from the gel. Due to the forms of self-assembled structures, like micelles, they can fuse with the lipid bilayers of the stratum corneum, thereby enhancing the partitioning of the entrapped drug as well as the disruption of the ordered bilayer structure [52]. The levels of MTZ release from $F5_{DMSO\text{-}MTZ}$, $F5_{EtOH\text{-}MTZ}$, and $F5_{TRANS\text{-}MTZ}$ were lower than that from $F5_{MTZ}$. Since the skin permeation of a drug is related to its release from formulations, a lower MTZ release should be related to lower skin permeation. Chemical compositions of the formulations also could influence the drug diffusivity and the release rate of the entrapped MTZ in its formulations. These results are supported by the flux and release rate calculated as shown in Tables 7 and 8. Further experiment would be needed to clarify the reason for the enhancement effect by CPEs incorporated Pal-GH gel formulations.

The treatment of many dermatological disorders relies on the penetration ability of active agents into the stratum corneum from applied formulations and their concentration in the viable epidermis and dermis layer [19]. The skin concentrations of MTZ were determined in the epidermis and dermis layer. The skin concentration of a topically applied drug has a very close relationship to its skin permeation [31], and in the steady-state, it can be expressed with

the product of the partition coefficient and the drug concentration. Thus, the increased MTZ concentration in VED in $F5_{PG\text{-}MTZ}$ and $F5_{IPM\text{-}MTZ}$ was derived from increased drug partitioning from the formulation into the stratum corneum. The enhancement ratios of MTZ concentration in the whole skin and in the stratum corneum were much higher than those in VED. This may be related to the difficulty in completely removing the topically applied formulation from the applied site. Thus, the MTZ concentration in skin as a whole and in the stratum corneum may be overestimated by the remaining drug formulation on the skin surface.

Fibrous structure in the Pal-GH gel was observed in $F5_{PG\text{-}MTZ}$, $F5_{DMSO\text{-}MTZ}$ and $F5_{EtOH\text{-}MTZ}$. Although $F5_{TRANS\text{-}MTZ}$ displayed fibrous structure, these three formulations seem to have distinct and large fibrous aggregates in their formulations compared with that in $F5_{TRANS\text{-}MTZ}$. Thus, PG, DMSO and EtOH in the gel formulations might be involved in the construction of micelle-like Pal-GH assemblies. Even though miscibility and the distribution of CPE in the inside and outside of the micelles would be related to the skin-penetration enhancement, the distribution of fibrous structures and their states in the Pal-GH gel might be a reason for the increased MTZ permeation through skin from the gel.

TEM observations were conducted to confirm the changes in the structures of the Pal-GH assemblies following the addition of several enhancers. The TEM results showed that the addition of PG, IPM, and DMSO to the Pal-GH formulation induced the morphological changes of fiber from the straight to twisted structures (Fig. 21b–d). These results suggest that

the structural differences of fibers may be related to the skin penetration-enhancement effect of the entrapped drug in the Pal-GH gel formulation. Furthermore, the thixotropic behavior of the Pal-GH gel was changed by the addition of CPEs. This behavior could be related to the microstructure of Pal-GH assemblies in the formulation. The increase in formulation velocity is likely to be related to the network structures of micelle-like Pal-GH assembly, because molecular–molecular interaction affects the gel structure stabilization [53]. Highly dense and twisted fibrous structures were probably correlated with the thixotropic behavior of Pal-GH gel formulations. Further experiments are required to clarify the exact reasons for the changing rheological behavior and enhancement effect by CPEs incorporated in Pal-GH gel formulations

The present study shed light on the possibility of Pal-GH gel formulations enhancing the skin permeation and concentration. However, detailed reasons for the enhancement mechanism in skin permeation following the application of Pal-GH gel formulations compared to those containing CPEs were not clearly revealed. Further studies are needed to understand the skin permeation enhancement effect in hydrophilic drugs by Pal-GH gels.

2.5. Chapter conclusion

In the present study, the skin permeation and concentration of MTZ improved following the application of Pal-GH as a formulation base. The addition of enhancers changed the molecular assembly of fibrous micelle-like of Pal-GH gel. These results illustrate that the

addition of additives/enhancers to the assembly amplified to induce the microscopic network structures, thereby alter the skin penetration-enhancement effect of the Pal-GH. Thus, the present findings are novel and should provide useful concepts in the development of supramolecular hydrogels having skin penetration-enhancement effects of drug. These results suggest that Pal-GH may have the potential to be used in dermatological formulations to improve their therapeutic efficacy, although elucidation of the enhancement mechanisms of Pal-GH gel and its constituent CPEs is necessary.

General Discussion

Pal-GH is a recently developed low molecular gelling agent, it is easy to synthesize and prepare because of its well-defined structure. Therefore, it is thermo-reversible and it can be re-dissolved. It has valuable properties like thixotropic behavior, lower viscosity and high dissolving properties for a wide range of hydrophilic to lipophilic drugs since it has hydrophilic and lipophilic sites (ambiphilic). No previous studies have utilized it in pharmaceutical application. Gelling agent having thixotropic behavior is an important consideration in preparing a gel spray formulation. Thixotropic gels can also be applied on a wider area of the skin for a long period. Pal-GH cannot only be used as a base for GS formulation due to its thixotropic properties, but also expected as a good enhancer [1, 2].

In the present study, we emphasized on designing a novel Pal-GH GS formulation containing IVM as a lipophilic model drug, and to observe the effects of Pal-GH gel formulation and its combination with several CPEs on the skin permeation and skin concentration of topically applied MTZ as a hydrophilic model drug. Thus, the design to use Pal-GH as a gelling agent for topically applied GS formulation containing IVM and also as enhancer for MTZ. Then, the understanding of the microstructures of Pal-GH in influencing thixotropic properties, enhancing skin permeation and skin concentration of the model drugs will be essential in developing superior topical formulations.

In this study, the strategy of the first chapter was focused on screening the physical characterizations and thixotropic properties of the prepared formulations in order to select and develop the best Pal-GH GS formulation. The author conducted the screening which was based on physical evaluation of Pal-GH gel formulations as follows: gel forming property after shaking, spraying ability, sprayed area, weight of sprayed formulation, and homogeneity. All formulations showed gel form after shaking, good homogeneity and spraying ability. Higher hysteresis areas (good thixotropic) were observed in Pal-GH containing PG. The thixotropic properties are influenced by several factors, one of them is by mixing with additives [28]. In general, the thixotropic property and physical characterization are very important factors that should be considered in designing GS formulation. Based on the screening, Pal-GH formulations with PG is the best candidate for the development of GS formulations containing IVM. Thus further experiments were conducted with these formulations ($F2.5_{4PG\text{-}IVM}$ and $F5_{4PG\text{-}IVM}$).

The *in vitro* release results of IVM from $F2.5_{4PG\text{-}IVM}$ and $F5_{4PG\text{-}IVM}$ showed that no significant differences were observed among all the tested Pal-GH formulations. Amount of IVM released from the PG solution was higher than that from the $F2.5_{4PG\text{-}IVM}$ and $F5_{4PG\text{-}IVM}$ (Fig. 7). The release of the entrapped molecules is dependent on the interaction with the gelling agent. These observations indicate that IVM is preferentially retained in the gel, presumably as a result of stronger interactions with the Pal-GH molecules. This phenomenon can be attributed

to van der Waals and hydrogen bonding interactions, which can also interact electrostatically with the Pal-GH. Moreover, the size of the pores between the fibers also play important role in the release of IVM. A significant improvement in skin concentration of IVM was observed with the application of $F2.5_{4PG\text{-}IVM}$ and $F5_{4PG\text{-}IVM}$ compared with IVM in PG (Fig. 8). These results suggest that the state of IVM, as well as its thermodynamic activity in the vehicle, affect the skin concentration of IVM. These results indicate that our developed Pal-GH GS formulation is a promising approach for enhancing the skin concentration of IVM (lipophilic model drug) after topical application.

In chapter 2, since the skin permeation rate of water soluble drugs is low in general, the author tried to use Pal-GH and its combination with several enhancers to increase the skin permeation and concentration of MTZ as a hydrophilic model drug after the topical application of Pal-GH gel. Microstructural observation was also conducted to observe the correlation between network structure of Pal-GH with skin-penetration enhancement effect and thixotropic properties. Based on the screening of the *in vitro* release and skin permeation of MTZ from different concentration of Pal-GH gels (Fig. 14a and b), the Pal-GH 5% was used to evaluate the effect of CPEs on the skin permeation and concentration of MTZ. Pal-GH itself ($F5_{MTZ}$) showed the skin-penetration enhancement effect (Fig. 16), and among the enhancers used in this chapter only IPM_{MTZ} showed the penetration enhancement effect (Fig. 13). The levels of MTZ permeation from combination of Pal-GH with PG, DMSO, and EtOH were higher than

that of the control solution. However, combination of Pal-GH with DMSO, EtOH and TRANS have decreased the skin-penetration enhancement effect of Pal-GH itself (Fig. 16). Contrarily, the combination of Pal-GH with PG and IPM showed a synergistic effect wherein they showed a significant increase in the skin penetration enhancement effect of Pal-GH itself. Thus, the skin concentration of Pal-GH and its combination with PG and IPM were evaluated. The increased MTZ concentration in VED was derived from increased drug partitioning from the formulation into the stratum corneum.

Since the Pal-GH gel had a fibrous structure in all formulations (Fig. 20 and 21) and MTZ in Pal-GH gel resulted in a change in the assembly from lamellar-like to micelle-like assemblies from the broad scattering SAXS pattern (Fig. 19), it was confirmed that micelle-like assemblies were formed by Pal-GH as an ambiphilic molecule [24]. Then, the construction of fibrous micelle-like Pal-GH assemblies may be a reason for the increase in MTZ permeation from the gel. Micelle-like assemblies in the Pal-GH gel might act as a drug carrier to have a high skin permeation of MTZ. However, miscibility and distribution of CPE in the inside or outside of the micelles also would affect the skin penetration-enhancement of MTZ. Due to the forms of self-assembled structures, like micelles, they can fuse with the lipid bilayers of the stratum corneum, thereby enhancing the partitioning of the entrapped drug as well as the disruption of the ordered bilayer structure [52]. Based on these result, we can conclude that assembly of Pal-GH in water as follows (Fig. 22):

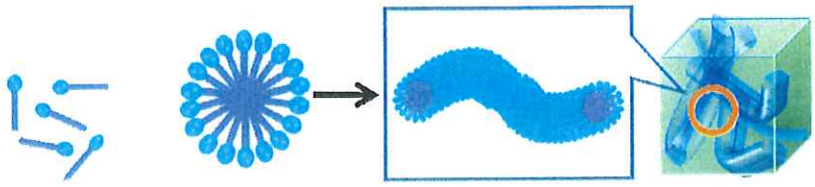

Fig. 22. Assembly of Pal-GH in water via non-covalent force (hydrogen-bonding, electrostatics, π-stacking etc) leads to the formation of fibrous structures. Entanglement of these fibers leads to a three dimensional network which immobilized the water.

Matsumoto *et al.* (2015) reported that Pal-GH combination with sodium palmitate results in a change in the assembly from lamellar-like to fibrous micelle-like. Consequently, sheet-shaped aggregates turn into flexible fibrils, forming bundles and resulting in a network structure. This phenomenon will affect the morphology and alter the bulk viscoelastic properties of hydrogel [24].

The TEM results showed that the addition of PG, IPM, and DMSO to the Pal-GH formulation induced the morphological changes of fiber from straight to twisted structures and higher amount of fiber (Fig. 21B-D). Microscopic data also showed distinct and large fibrous aggregates for these three formulation compared to the addition of TRANS. These results suggest that the higher amount and twisted structural fibers may be related to increasing the skin penetration-enhancement effect of the entrapped drug in the Pal-GH gel formulation.

Highly dense, fragmented shape and twisted fibrous structures were probably correlated with the thixotropic behavior of Pal-GH gel formulations. However, detailed reasons for the correlation between thixotropic behavior and skin-penetration enhancement effect were not clearly revealed. Further experiments are required to clarify the exact reasons for the changing rheological behavior and enhancement effect by CPEs incorporated in Pal-GH gel formulations.

Conclusion

From these results obtained above, the following conclusions were obtained:

1. The Pal-GH has valuable properties as a base of topical applied gel formulation especially for gel spray formulation.
2. Pal-GH and a combination of Pal-GH with PG and IPM are potential candidates to enhance skin permeation and skin concentration of lipophilic and hydrophilic drugs.
3. The changing in the assembly of Pal-GH hydrogel from lamellar-like to fibrous micelle-like consequently, structural differences, higher amount of fibers and twisted fiber structure may be related to the skin penetration-enhancement effect of the entrapped drug in the Pal-GH gel formulation.
4. Highly dense, fragmented shape and twisted fibrous structures were found to be correlated with thixotropic behavior of Pal-GH gel formulations.
5. Further studies should be performed to clarify the detail correlation between gel thixotropic properties and skin penetration enhancement effect of Pal-GH assembly.
6. This approach may enhance skin permeation of mal-absorptive drugs and provide insight in formulating superior topical formulations.

Acknowledgements

It is a pleasure to thank many people who made this dissertation possible. I would like to express my sincere gratitude to my Ph.D. supervisor, Professor Kenji Sugibayashi and Assoc. Professor Dr. Hiroaki Todo, for their valuable discussion and suggestion through the present research. With their enthusiasm, their inspiration, and their great efforts to explain things clearly and simply, they helped to make research work easier for me. Throughout my dissertation-writing period, they provided encouragement, sound advice, good teaching, philosophy thinking, and lots of good idea. I would have been lost without them. I am especially grateful to Prof. Hideshi Natsume, Prof. Shoichiro Ohta and Prof. Tomomi Hatanaka, for valuable suggestions to make this research meaningfully. Also I am grateful to Professor Konstanty Wiertzba and Dr. Wesam Radhi Kadhum, for helping me to overcome the communication barrier, get through the difficult times in my daily life in Japan. I also wish to thank all other colleagues who helped me especially ms. Mika Futaki, ms. Akie Okada and all of master course students in the Laboratory of Pharmaceutics and Cosmeceutics.

Lastly I am grateful to Ministry of Religious Affairs Republic of Indonesia who gives me this opportunity to come to Japan to carry out the present study by MORA (Ministry of Religious Affairs) overseas Ph.D Scholarship.

The most importantly, I also wish to express my deep gratitude to my husband, Novan

Ham Lelo Batuah, my soul, for his continual love, kindly encouragement, and endless support, who always stand beside me through difficult part of my life, who always wait patiently to face me, who always be a good leader and advisor for me, who always love me with all of my weaknesses, for his understanding, for his supporting, love you much before, now and forever In syaa Allah.

I am forever indebted to my parents, Asmidar Darwis and Dahlizar Dahlan, and my parents in law, Syamsinar Johar Kamin and Hasmi Ham. They raised me, supported me, taught me and loved me. I am also grateful for all of my daughters, Syiva Annajla, Salma Auva Riadha, and Sarah Nazhiva, who always support me with their cheers, always make me happy during this periode.

Lastly, I wish to thank to Nissan Chemical Industries, Ltd. (Tokyo, Japan) for the supporting materials for the present study.

References

1) Ohsedo Y., Low-molecular-weight gelators as base materials for ointments. *Gels,* **2**, 1–13 (2016).

2) Sabrina D., Futaki M., Okada A., Kadhum W.R., Todo H., Sugibayashi K., Design of a topically applied gel spray formulation with ivermectin using a novel low molecular weight gelling agent, palmitoyl-glycine-histidine, to treat scabies. *Chem. Pharm. Bull.*, **66**, 1–8 (2018).

3) Cross S.E., Roberts M.S., The effect of occlusion on the epidermal penetration of parabens from a commercial test ointment, acetone and ethanol vehicles. *J. Invest. Dermatol.*, **115**, 914–918 (2000).

4) Asbill C.S., Michniak B.B., Percutaneous penetration enhancers: local versus transdermal activity. *Pharm. Sci. Technol.*, **3**, 36–41 (2000).

5) Li J. L., Liu X. Y., architecture of supramolecular soft functional materials : from understanding to micro-/nanoscale engineering. *Adv. Funct. Mater.*, **20**, 3196–3216 (2010).

6) Krieg E., Shirman E., Weissman H., Shimoni E., Wolf S. G., Pinkas I., Rybtchinski B., Supramolecular gel based on a perylene diimide dye: multiple stimuli responsiveness, robustness, and photofunction. *J. Am. Chem. Soc.*, **131**, 14365–14373 (2009).

7) Lee K. Y., Mooney D. J., Hydrogels for tissue engineering. *Chem. Rev.*, **101**, 1869–1879

(2001).

8) Saboktakin M. R., Tabatabaei R. M., Supramolecular hydrogels as drug delivery system. *Int. J. Biol. Macromol.*, **75**, 426–436 (2015).

9) Hay R. J., Steer A. C., Engelman D., Walton S., Scabies in the developing world—its prevalence, complications and management. *Clin. Microbiol. Infect.*, **18**, 313–323 (2012).

10) Haas N., Lindeman U., Frank K., Sterry W., Lademann J., Katzung W., Rapid and preferential sebum secretion of ivermectin: a new factor that may determine drug responsiveness in patients with scabies. *Arch. Dermatol.*, **138**, 1618–1619 (2002).

11) Currie B. J., McCarthy J. S. N., Permethrin and ivermectin for scabies. *Engl. J. Med.*, **362**, 717–725 (2010).

12) Hicks M. I., Elston D. M., Scabies. *Dermatol. Ther.*, **22**, 279–292 (2009).

13) Fawcett R. S., Ivermectin use in scabies. *Am. Fam. Physician,* **68**, 1089–1092 (2003).

14) Miyajima A., Komoda M., Akagi K., Yuzawa K., Yoshimasu T., Yamamoto Y., Hirota T., Pharmacokinetics of ivermectin applied topically by whole-body bathing method in healthy volunteers. *J. Dermatol.*, **42**, 87–89 (2015).

15) Levi A., Mumcuoglu K. Y., Ingber A., Enk C. D., Assesment of *sarcoptes scabiei* viability *in vivo* by reflectance confocal microscopy. *Lasers Med. Sci.*, **26**, 291–292 (2011).

16) Goldust M., Golforoushan F., Rezaee E., Treatment of solar lentigines with trichloroacetic acid 40% vs cryotheraphy. *Eur. J. Dermatol.*, **21** 426–427 (2011).

17) Heukelbach J., Feldmeier H., Scabies. *Lancet*, **367**, 1767-1774 (2006).

18) Mewis J., Wagner N. J., Thyxotropy. *Adv. Colloid Interface Sci.*, **14**, 214–227 (2009).

19) Watanabe T., Hasegawa T., Takahashi H.; Ishibashi, T.; Takayama, K.; Sugibayashi, K., Utility of three-dimensional cultured human skin model as a tool to evaluate skin permeation of drugs. *Altern. Anim. Test Exp.*, **8**, 1–14 (2011).

20) Morimoto Y., Hatanaka T., Sugibayashi K., Omiya H., Prediction of skin permeability of drugs: comparison of human and hairless rat skin. *J. Pharm. Pharmacol.* **44**, 634–639 (1992).

21) Abd E., Yousef S.A., Pastore M.N., Telaprolu K., Mohammed Y.H., Namjoshi S., Grice J.E., Roberts M.S., Skin models for testing of transdermal drugs. *Clin. Pharmacol. Adv. App.*, **8**, 163–176 (2016).

22) Jung E.C., Maibach H.I., Animal models for percutaneous absorption. *J. Appl. Toxicol.*, **35**, 1–10 (2015).

23) Anderson R.L., Cassidy J.M., Variation in physical dimension and chemical composition of human stratum corneum. *J. Invest. Dermatol.*, **61**, 30-32 (1973).

24) Matsumoto K., Shundo A., Ohno M., Fujita S., Saruhashi K., Miyachi N., Miyaji K., Tanaka K., Modulation of physical properties of supramolecular hydrogels based on a hydrophobic core. *Phys. Chem. Chem. Phys.*, **17**, 2192–2198 (2015).

25) Goldust M., Rezaee E., Raghivar R., Hemayat S., Treatment of scabies: the topical

ivermectin vs permethrin 2.5% cream. *Ann. Parasitol.*, **59**, 79–84 (2013).

26) Deeks L.S., Naunton M., Currie M.J., Bowden F.J., Topical ivermectin 0.5% lotion for treatment of head lice. *Ann. Pharmacother.*, **47**, 1161–1167 (2013).

27) Sangeetha N. M., Maitra U., Supramolecular gels; fuctions and uses. *Chem. Soc. Rev.*, **34**, 821–836 (2005).

28) Barry B.W., Thixotropic property in pharmaceutical formulations. *J. Texture Stud.*, **1**, 405–430 (2007).

29) Kunst A., Lee G., Release and skin permeation of scopolamine from thin polymer films in relation to thermodynamic activity. *J. Pharm. Sci.*, **105**, 1496–1500 (2016).

30) Daraio M.E., Francois N. J., Bernik D. L., Correlation between gel structural properties and drug release pattern in scleroglucan matrices. *Drug Deliv.*, 10, 79–85 (2003).

31) Sugibayashi K., Todo H., Oshizaka T., Owada Y., Mathematical model to predict skin concentration of drugs: toward utilization of silicone membrane to predict skin concentration of drugs as an animal testing alternative. *Pharm. Res.*, **27**,134–142 (2010).

32) Asbill C.S., El-Kattan A.F., Michniak B., Enhancement of transdermal drug delivery: Chemical and physical approaches. *Crit. Rev. Ther. Drug Carrier Syst.*, **17**, 621–658 (2000).

33) Barrett C.W., Hadgraft J.W., Caron G.A., Sarkany I., The effect of particle size on the percutaneous absorption of fluocinolon acetonide. *J. Dermatol.*, **77**, 575–578 (1965).

34) Coldman M.F., Poulsen, B. J., Higuchi, T., Enhancement of percutaneous absorption by the use of volatile: nonvolatile system as vehicles. *J. Pharm. Sci.,* **58**, 1098-1102 (1969).

35) Hoelgaard A., Mollgaard B., Dermal drug delivery-improvement by choice of vehicle or drug derivative. *J. Control. Release*, **2**, 111–120 (1985).

36) Nicolazzo J.A., Morgan T.M., Reed B.L., Finnin B.C., Synergistic enhancement of testosterone transdermal delivery. *J. Control. Release*, **103**, 577–585 (2005).

37) Kurihara-Bergstrom T., Knutson K., DeNoble L., Goates C.Y., Percutaneous absorption enhancement of an ionic molecule by ethanol-water systems in human skin. *Pharm. Res.*, **7**, 762-776 (1990).

38) Leopold C.S., Lippold B.C., An attempt to clarify the mechanism of the penetration enhancing effects of lipophilic vehicles with differential scanning calorimetry (DSC). *J. Pharm. Pharmacol.*, **47**, 276–281 (1995).

39) Harrison J.E., Watkinson A.C., Green D.M., Hadgraft J., Brain K., The relative effect of Azone and Transcutol on permeant diffusivity and solubility in human stratum corneum. *Pharm. Res.*, **13**, 542–546 (1996).

40) Roth S.H., Fuller P., Diclofenac sodium topical solution 1.5% w/w with dimethyl sulphoxide compared with placebo for the treatment of osteoarthritis; pooledsafety results. *Postgrad. Med.*, **123**, 180–188 (2011).

41) Thong H.Y., Zhai H., Maibach H.I, Percutaneous penetration enhancers: an overview.

Skin Pharmacol. Physiol., **20**, 272–282 (2007).

42) Zafar S., Ali A., Aqil M., Ahad A., Transdermal drug delivery of labetalol hydrochloride: Feasibility and effect of penetration enhancers. *J. Pharm. Bioallied Sci.*, **2**, 321–324 (2010).

43) Marren, K., Dimethyl sulfoxide: An effective penetration enhancer for topical administration of NSAIDs. *Phys. Sportsmed.*, **39**, 75–82 (2011).

44) Scheuplein R.J., Blank I.H., Permeability of the skin. *Physiol. Rev.*, **51**, 702–747 (1971).

45) Sekura D.L., Scala J., The percutaneous absorption of alkyl methyl sulfoxides. *Adv. Biol. Skin,* **12**, 257–269 (1972).

46) Mills P.C., Vehicle effects on the *in vitro* penetration of testosterone through equine skin. *Vet. Res. Commun.*, **31**, 227–233 (2007).

47) Gee C.M., Watkinson A.C., Nicolazzo J.A., Finnin B.C., 2014. The effect of formulation excipients on the penetration and lateral diffusion of ibuprofen on and within the stratum corneum following topical application to humans. *J. Pharm. Sci.*, **103**, 909–919 (2014).

48) Kietzmann, M., Blume, B., Percutaneus absorption of betamethasone from different formulations using the isolated perfused bovine udder. *In Vitro Toxicol.*, **10**, 11–15 (1997).

49) Herai H., Gratieri T., Thomazine J.A., Bentley M.V., Lopez R.F., Doxorubicin skin penetration from monoolein-containing propylene glycol formulations. *Int. J. Pharm.*, **32**, 88–93 (2007).

50) Mollgaard B., Hoelgaard A., Vehicle effect on topical drug delivery. I. Influence of glycols and drug concentration on skin transport. *Acta Pharm. Suec.*, **20**, 433–442 (1983).

51) Hirvonen J., Rajala R., Vihervaara P., Laine E., Paronen P., Urtti A., Mechanism and reversibility of penetration enhancer action in the skin. *Eur. J. Pharm. Biopharm.*, **40**, 81–85 (1995).

52) Karande P., Mitragotri S., Enhancement of transdermal drug delivery *via* synergistic action of chemicals. *Biochim. Biophys. Acta,* **11**, 2362–2373 (2009).

53) Mallia V.A., Weiss R.G., Correlations between thixotropic and structural properties of molecular gels with crystalline networks. *Soft Matter*, **12,** 3665–3676 (2016).